A block-structured model for banking networks across multiple countries

Janina Engel[1], Andrea Pagano[1], Matthias Scherer[2]

Abstract A block-structured model for the reconstruction of directed and weighted financial networks, spanning multiple countries, is developed. In a first step, link-probability matrices are derived via a fitness model that is calibrated to reproduce a desired density and reciprocity for each block (i.e. country and cross-border sub-matrix). The resulting probability matrix allows for fast simulation through bivariate Bernoulli trials. In a second step, weights are allocated to a sampled adjacency matrix via an exponential random graph model (ERGM), which fulfills the row, column, and block weights. This model is analytically tractable, calibrated only on scarce publicly available data, and closely reconstructs known network characteristics of financial markets. In addition, an algorithm for the parameter estimation of the ERGM is presented. Furthermore, calibrating our model to the EU interbank market, we are able to assess the systemic risk within the European banking network by applying various contagion models.

Keywords: financial network reconstruction; fitness model; exponential random graph model; maximum entropy; systemic risk.

AMS 2010 Subject Classification: 05C80, 90B15.

Acknowledgment We are grateful to Diego Garlaschelli and Tiziano Squartini for their valuable input and their suggestions regarding the model presented in this paper. Also, we want to thank Stefano Battiston, Guido Caldarelli, Marco D'Errico, Stefano Gurciullo, Alan Roncoroni and Gabriele Visentin for providing the code of the "FINEXUS Leverage Network Framework for Stress-testing".

[1]European Commission, Joint Research Centre (JRC), Directorate Growth and Innovation, Finance and Economy Unit, Via Enrico Fermi 2749, 21027 Ispra (VA), Italy

[2]Chair of Mathematical Finance, Technical University of Munich, Parkring 11, 85748 Garching, Germany

1. Introduction

The global financial crisis of 2007–2008 highlighted the need for a deeper understanding of our financial markets and an accurate assessment of systemic risk [40]. In 2010, the Basel Committee on Banking Supervision [39] identified the interconnectedness of financial institutions as a significant source of systemic risk and an important cause for a further amplification of the crisis. Moreover, at the time of the crisis, authorities' stress tests failed to adequately model interlinkages in the banking sector, which in turn led to a dramatic underestimation of the vulnerability of financial systems [40].

Since then, the literature on systemic risk measuring has gained great attention. Early research includes work by Allen and Gale (2000) [2], who construct market equilibria between banks and consumers and analyze the contagion of liquidity shocks to the system. Based on examples of networks containing only four banks, forming either a completely connected graph or a circle, they conclude that completely connected graphs are less fragile than circles. Eisenberg and Noe (2001) [22] developed a clearing mechanism that is very popular today, i.e. they constructed a payment vector for the nodes of a financial system that is based on a proportional propagation of losses among counterparties. While Eisenberg and Noe reallocate the initial loss of a defaulting bank (i.e. the total resulting loss has always the exact same size as the initial loss), Cifuentes et al. (2005) [14] add losses in equity caused by price drops of illiquid assets. Based on simulations of networks of ten homogeneous banks, the authors conclude that systemic resilience and bank interconnections are not linearly related and that in particular circumstances more interconnected networks may be riskier (which is not in line with the results of Allen and Gale (2000) [2]). Recently, contagion mechanisms and systemic risk measures have been further extended and new ideas have been suggested. For example, Rogers and Veraart (2013) [43] generalized the model of Eisenberg and Noe by introducing default costs. Battiston et al. (2012) [11, 9] proposed the so-called *DebtRank* as a measure of systemic impact, that is based on the idea of feedback-centrality. Cont et al. (2013) [17] developed a simulation-based approach named the *Contagion Index* that quantifies the expected loss in capital generated by an institutions default in the light of a recovery rate of zero.

For a detailed survey on systemic risk models, the interested reader is referred to De Bandt and Hartmann (2000) [20] and Hüser (2015) [31]. While this strand of literature keeps growing, the problem of constructing realistic models of financial networks remains open. This is a challenging task, because information on bilateral interbank-activities is classified confidential and thus mostly not available. For a detailed discussion on the sparsity of consistent bank-level data, see Cerutti at al. (2011) [13]. The relevance of this issue has also been acknowledged by authorities, who in response launched several initiatives to fill essential data gaps, see, e.g., the G20 Data Gaps Initiative (DGI)[3] and the EU-wide transparency exercise by the European Banking Authority (EBA)[4]. Nonetheless, until today only few data on aggregated levels have been published.

Because of the lack of publicly available information on interbank lending, academics often turn to random graphs or toy networks to apply their developed tools. This allows to derive theoretical results on systemic risk for very specific and well controlled network structures. For a better understanding of the complex topology of actual financial markets, however, and its mechanism to propagate shocks, more realistic network models are needed. The formulation of tractable network models that (a) cover multiple countries, (b) allow for fast simulation of sample scenarios, (c) can be calibrated to available information, and thus generate realistic financial markets, and (d) offer the flexibility to easily change particular network characteristics for a detailed analysis, still remains an open challenge.

To fill this gap, we present an analytically tractable network reconstruction methodology, comprising each of the listed features (a) – (d) at least to some extend. Our model is based on earlier work [24] regarding the reconstruction of the topology of interbank networks of single countries. In the present work, we extend this model to cover multiple countries by using a block structure of weighted networks. More precisely, in a first step we use an extended fitness model to reconstruct the adjacency matrix of the underlying financial network, calibrated to a desired density and reciprocity. This results in a link-probability

[3]For more information see e.g. `http://www.imf.org/external/np/seminars/eng/dgi/`.

[4]For more information see `http://www.eba.europa.eu/risk-analysis-and-data/eu-wide-transparency-exercise`.

matrix from which we can easily sample adjacency matrices through bivariate Bernoulli trials. In a second step, the sampled adjacency matrices are weighted, such that interbank assets and liabilities, which are known from the banks' balance sheets, as well as the total weight circulating within and across countries, is met. This is achieved via an exponential random graph model (ERGM), conditioned on the row and column sums as well as on the block weights. Since this model allows to analytically derive the expected weight of each link of a given adjacency matrix, the conditions are fulfilled exactly by the resulting network.

Our network reconstruction model enables the application of the proposed contagion mechanisms and systemic risk measures to more realistic and international financial networks. We expect the outcomes to shed new light on systemic risk and its monitoring. Furthermore, this analysis can also pave the way for further improvements on contagion models and systemic risk measures, as well as support the ultimate aim of policy-makers to stabilize financial markets.

This paper is structured as follows. Section 2 surveys existing network reconstruction methods, while Section 3 presents our extension. Since model calibration is a non-trivia task, Section 4 introduces an algorithm for parameter estimation in the present setup. In Section 5 we calibrate our model to the EU interbank market and characterize the resulting topology. Afterwards, in Section 6 we assess systemic risk in the EU interbank market by applying five of the most popular contagion mechanisms. The final Section 7 concludes and highlights open questions for further research.

2. Literature review on network reconstruction methods

An overview of the most prominent methods that have been suggested for recovering network structures from scarce data is presented in the following. A comparison of various models has been conducted by the Basel Committee on Banking Supervision [41], Mazzarisi and Lillo [35], and Anand et al. [5], generally concluding that the performance of each approach depends heavily on the underlying network structure.

As interbank assets and liabilities are publicly available through the banks' balance sheets, the primary problem for financial network reconstruction concerns the generation of matrices with zero-diagonal, i.e. excluding self-loops, that match the given row and column sums. One of the first approaches to tackle this issue was provided by Upper and Worms [51], who suggested a maximum entropy (ME) model. Because of the lack of further information, they propose to distribute the weights as uniform as possible. This is done by minimizing the Kullback–Leibler divergence w.r.t. the uniform distribution, while ensuring a zero diagonal as well as the desired row and column sums. A drawback of this approach is that the resulting network is completely connected, which contradicts most real-world financial networks that are typically sparse. Moreover, in some cases the ME model has been shown to underestimate systemic risk [36]. To reduce the density of the generated networks, changes on the uniform prior have been suggested. For example, Drehmann et al. [21] fix a random set of elements of the prior matrix to zero, and Baral and Fique [6] propose a Gumbel copula fitted to the marginals as prior.

Building on the ME approach, so called 'exponential random graph models' (ERGMs) or 'configuration models,' have been developed, which are able to incorporate further network characteristics, see for example [42, 48]. The idea is to construct a probability distribution over a set of graphs, again by minimizing the Kullback–Leibler divergence to the uniform distribution, while constraining the optimization problem on the expected value of certain desired network statistics. An advantage of these models is that constraints allowing for dyad independence, such as a desired density, degree sequence, reciprocity, in- and out-strength, etc., render the optimization problem analytically solvable. The flexibility in the constraints and the considered set of graphs gives rise to a number of different models. For example, Mastrandrea et al. [33] use an ERGM constrained on the degree and strength sequence to reconstruct a number of networks from different fields.

In contrast to the ME model, Anand et al. [4] address the opposed problem of creating networks with a minimum number of links, such that given row and column sums are met. In addition, they provide an extension for generating disassortative networks as well as a heuristic procedure for sampling. As they report, their model tends to overestimate systemic risk.

Another strand of literature concerns fitness models. Here, connections are generated according to a link probability function that depends on hidden variables of the respective nodes. For example, Cimini et al. [16] suggest to use available economic factors as hidden variables, such as the nodes' strengths, and a link probability function coming from an ERGM constrained on the in- and out-degree sequence. By introducing a scalar factor, multiplied with the hidden variables, the density of the resulting networks can be controlled. Sampling unweighted networks is fast and easy by drawing independent Bernoulli trails. Subsequently, weights are allocated via a gravity model.

A similar approach is presented by Gandy and Veraart [25, 26], who consider the same fitness model for the generation of the adjacency matrix as Cimini et al. [16], but suggest a Gibbs sampler for weight allocation. The MCMC sampler creates a sequence of weighted networks that all match the row and column sums exactly, and that converges to an exponential distribution w.r.t. the weights. Moreover, Gandy and Veraart also consider the reverse case of randomly distributed fitness variables and fitting a link probability function such that a power law degree distribution is achieved.

Hałaj and Kok [29], on the other hand, make use of additional information disclosed by the EBA's EU-wide stress test (see `http://www.eba.europa.eu`), comprising country level exposures of 89 banks. Based on this data, they derive the relative distribution of interbank exposures, aggregated on country level, which then serves as a link probability map. In an iterative procedure links are drawn at random and kept according to the derived probability map. Weights are allocated to sampled links by a uniformly distributed random fraction of unallocated weight. Once the total weight is assigned, the procedure terminates.

Our approach combines several aspects of the discussed methodologies. First, we use a fitness model to construct adjacency matrices, i.e. unweighted directed graphs. In the spirit of Cimini et al. [16] and Gandy and Veraart [26], our fitness model accounts for the nodes' heterogeneity and can be calibrated to a desired density. In addition, we incorporate degree reciprocity, i.e. the generated link probability matrix will match a desired number of reciprocal links. Similar to Hałaj and Kok [29] we make use of the EBA's EU-wide tranparency excercise (see `http://www.eba.europa.eu`) to estimate the distribution of interbank assets within countries and across borders. Since the data published by the EBA is incomplete, we use the estimated distribution as a prior in an ERGM, i.e. missing interbank assets are distributed as homogeneously as possible, while fulfilling the margins. In a last step, we use an ERGM with constraints on the row sums, column sums, and cross border weights to allocate weights to a sampled adjacency matrix. This ERGM differs from existing ERMGs in its constraints and the set of considered graphs.

3. Method

This section derives a block-structured probabilistic model for the reconstruction of international financial networks. We start with a precise description of the problem and of the desired model characteristics.

3.1. Problem of financial network reconstruction

In the following, we consider a network consisting of n financial institutions that are located in N countries, which are denoted by $C_1, C_2, \ldots, C_N$; $|C_j|$ denoting the number of banks in country $j \in \{1, \ldots, N\}$. This creates a chessboard with N^2 blocks. The corresponding network can be visualized in form of a matrix w, as illustrated in Fig. 1. The element w_{ij} equals the nominal value of loans that bank i lends to bank j. Consequently, the row sum $s_i^{(out)}$ (resp. column sum $s_i^{(in)}$) denotes the total interbank assets (resp. deposits) of bank i.

$$
w = \begin{array}{cc} & \begin{array}{cccc|cccc|ccc|ccc} & C_1 & & & & C_2 & & & & \dots & & & C_N & \\ b_1 & b_2 & \dots & b_{|C_1|} & b_{|C_1|+1} & \dots & \dots & b_{|C_1|+|C_2|} & \dots & \dots & \dots & b_{1+\sum_{j=1}^{N-1}|C_j|} & \dots & b_n \end{array} \\ \begin{array}{cc} & b_1 \\ & b_2 \\ C_1 & \vdots \\ & b_{|C_1|} \\ & \vdots \\ C_2 & \vdots \\ & \vdots \\ & \vdots \\ \vdots & \vdots \\ & \vdots \\ C_N & \vdots \\ & b_n \end{array} & \left(\begin{array}{cccc|cccc|ccc|ccc} 0 & \square & \dots & \square & \square & \dots & \dots & \square & & & & & & \\ \square & 0 & & \square & \square & \dots & \dots & \square & & & & & & \\ \vdots & & \ddots & \vdots & \vdots & & & \vdots & & & & & & \\ \square & \square & \dots & 0 & \square & \dots & \dots & \square & & & & & & \\ \hline & & & & \ddots & & & & & & & & & \\ & & & & & \ddots & & & & & & & & \\ & & & & & & \ddots & & & & & & & \\ & & & & & & & \ddots & & & & & & \\ \hline & & & & & & & & \ddots & & & & & \\ & & & & & & & & & \ddots & & & & \\ & & & & & & & & & & \ddots & & & \\ \hline & & & & & & & & & & & \ddots & & \\ & & & & & & & & & & & & \ddots & \\ & & & & & & & & & & & & & 0 \end{array}\right) \begin{array}{c} s_1^{(out)} \\ s_2^{(out)} \\ \vdots \\ \vdots \\ \vdots \\ \vdots \\ \vdots \\ \vdots \\ \vdots \\ \vdots \\ \vdots \\ s_n^{(out)} \end{array} \\ & \begin{array}{cccccccccccccc} s_1^{(in)} & s_2^{(in)} & \dots & \dots & \dots & \dots & \dots & \dots & \dots & \dots & \dots & \dots & \dots & s_n^{(in)} \end{array} \end{array} \tag{1}
$$

Figure 1: Illustration of an international financial network comprising n financial institutions $b_1, \dots, b_n$, grouped by their country of origin $C_1, \dots, C_N$. The variables $s_i^{(out)}$ and $s_i^{(in)}$ denote the i-th row and column sum, respectively.

As pointed out in the discussion above, the fundamental problem of reconstructing financial networks is the limited data availability. In fact, regarding interbank networks, the only information which is regularly available to the public are interbank assets $s^{(out)}$ and interbank liabilities $s^{(in)}$ of each bank. However, considering all networks which fulfill the given row and column sums as possible financial networks is misleading, since financial networks are, for example, known to be sparse, see, e.g., Craig and Peter [19]. Hence, densely connected networks should be excluded on the grounds of not being realistic. Moreover, financial networks are known to be disassortative, to exhibit a core-periphery structure, to feature short paths, degrees and strength are highly correlated, etc., see, e.g., Craig and Peter [19], Roukny et al. [45], Bargigli et al. [8]. But precise, regular, and complete information on theses characteristics are not publicly available. Thus, to construct realistic networks, a trade-off has to be made on incorporating available data and accuracy of the reconstructed network topology. Furthermore, we aim at a tractable model which also includes the flexibility to change particular network statistics, in order to allow for a detailed assessment of systemic risk and an analyses of potentially more stable network structures. Therefore, we choose to base our model on the following characteristics (i) - (iv) for two reasons. First, the necessary information is either publicly available or can be approximated from publicly available data, as demonstrated in Section 5.1 w.r.t. the EU interbank network. This allows the construction of realistic interbank networks. Second, these characteristics can be incorporated in an analytically tractable model. Hence, these characteristics can easily be twisted and network ensembles with different structures can be generated. This creates a flexible playground for a detailed analysis on systemic risk and possible new regulations, which is a key objective of this work. We assume the following information to be given:

(i) The density for each block, or equivalently the number of links $L_{kl}^{\rightarrow}$ for all blocks $k, l = 1, \dots, N$, i.e.

$$L^{\rightarrow} \in \mathbb{N}_0^{N \times N}; \tag{2}$$

(ii) The (degree-) reciprocity for each pair of transposed blocks, or equivalently the number of mutual links $L_{kl}^{\leftrightarrow} = L_{lk}^{\leftrightarrow}$ for all blocks $k, l = 1, \dots, N$, i.e.

$$L^{\leftrightarrow} \in \mathbb{N}_0^{N \times N}, \text{ and } L^{\leftrightarrow} \text{ symmetric}; \tag{3}$$

(iii) Interbank assets $s_i^{(out)}$ and liabilities $s_i^{(in)}$ for each bank $i = 1, \dots, n$ in the network, i.e.

$$s^{(in)} \in \mathbb{N}_0^n \quad \text{and} \quad s^{(out)} \in \mathbb{N}_0^n; \tag{4}$$

(iv) The total weight for each block, i.e.

$$s^{(block)} \in \mathbb{N}_0^{N\times N}. \tag{5}$$

The row and columns sums, as well as the block weights, are restricted to the set of natural numbers, as this considerably simplifies the required calculations, see Section 3.3.

Following the notation of Gandy and Veraart [25], let $w \in \mathbb{N}_0^{n\times n}$ denote an interbank matrix, where the element w_{ij} denotes the nominal value of interbank loans granted from bank i to bank j. Some stakeholders, such as financial institutions, central banks, or regulators might have partial knowledge on the interbank network, i.e. they might know the true value of some elements of w. Therefore, we define $w^* \in \mathcal{W} := (\{*\} \cup \mathbb{N}_0)^{n\times n}$, where $w^*_{ij} = *$ denotes an unknown matrix element. We are interested in the set of all interbank matrices fulfilling the desired characteristics (i) – (iv), as well as matching all known bilateral interbank elements. Constructing this set of matrices in a tractable and computationally feasible way is a non-trivial task, and to the best of our knowledge such a model is currently not yet available. To provide a solution, we relax the problem and consider instead a probability space that generates interbank matrices which satisfy the desired characteristics in expectation.

Definition 3.1 (Admissible probability space for interbank networks)
Let $\Omega := \left\{w \in \mathbb{N}_0^{n\times n}\right\}$ be a set of weighted and directed graphs and let $P : \mathfrak{P}(\Omega) \to [0,1]$ be a probability measure defined on the power set $\mathfrak{P}(\Omega)$ of Ω . The probability space $(\Omega, \mathfrak{P}(\Omega), P)$ is called admissible *w.r.t. $L^{\to} \in \mathbb{N}_0^{N\times N}$, $L^{\leftrightarrow} \in \mathbb{N}_0^{N\times N}$ symmetric, $s^{(in)} \in \mathbb{N}_0^n$, $s^{(out)} \in \mathbb{N}_0^n$, $s^{(block)} \in \mathbb{N}_0^{N\times N}$, and w^* if the following conditions are met:*

(i)

$$\sum_{w\in\Omega} P(w) \left[\sum_{i\in C_k, j\in C_l} \mathbb{1}_{\{w_{ij}>0\}} \right] = L^{\to}_{kl}, \quad \forall k,l = 1,\dots,N, \qquad \text{(directed links)}$$

(ii)

$$\sum_{w\in\Omega} P(w) \left[\sum_{i\in C_k, j\in C_l} \mathbb{1}_{\{w_{ij}>0\}} \mathbb{1}_{\{w_{ji}>0\}} \right] = L^{\leftrightarrow}_{kl}, \quad \forall k,l = 1,\dots,N, \qquad \text{(reciprocal links)}$$

(iii)

$$\sum_{w\in\Omega} P(w) \left[\sum_{j=1}^{n} w_{ij} \right] = s_i^{(out)}, \quad \forall i = 1,\dots,n, \qquad \text{(assets)}$$

(iv)

$$\sum_{w\in\Omega} P(w) \left[\sum_{i=1}^{n} w_{ij} \right] = s_j^{(in)}, \quad \forall j = 1,\dots,n, \qquad \text{(liabilities)}$$

(v)

$$\sum_{w\in\Omega} P(w) \left[\sum_{i\in C_k, j\in C_l} w_{ij} \right] = s_{kl}^{(block)}, \quad \forall k,l = 1,\dots,N, \qquad \text{(block weights)}$$

(vi)

$$w_{ij} = w^*_{ij}, \quad \forall w \in \Omega \text{ and } w^*_{ij} \neq *. \qquad \text{(known links)}$$

In the following, we present a model for generating such admissible ensembles of interbank matrices.

3.2. Reconstructing unweighted directed graphs via an extended fitness model

Fitness models have been studied in detail by, e.g., Caldarelli et al. [12], Servedio et al. [46], Musemci et al. [37], and Gandy and Veraart [25]. We only summarize the particular fitness model that we use for our purposes.

Fitness models are based on the assumption that the link probability is controlled by underlying node specific hidden variables. While one strand of literature randomizes the hidden variables and derives link probability functions, such that some desired characteristics are fulfilled, another strand uses given economic factors as hidden variables. We adopt the latter methodology. More precisely, we take the link probability function as given by an ERGM conditioned on the in- and out-degree sequences and the number of reciprocal links. For a derivation of this ERGM, see, e.g., Engel et al. [24] and the references therein.

The parameters of the ERGM can be estimated for a given in- and out-degree sequence and a given number of reciprocal links. For most blocks, however, no information on the in- and out-degrees is publicly available. For this reason, we resort to the idea of fitness models and consider the unknown parameters (i.e. the exponential function of the negative Lagrange multipliers) as hidden variables. More precisely, the hidden variables controlling the link probabilities are specified by the banks' interbank assets $s_i^{(out)}$ and interbank liabilities $s_i^{(in)}$, multiplied by a block specific parameter $z \in \mathbb{R}_{\geq 0}^{N\times N}$ that controls for the network density of each block. This leads to the following link probabilities: Let $A \in \{0,1\}^{n\times n}$ denote the random adjacency matrix, and to simplify notation let z_{ij} denote the z parameter of the corresponding block, then for $i \neq j$,

$$P\left(A_{ij} = 1 \wedge A_{ji} = 1\right) = \frac{r_{ij}^2 z_{ij} z_{ji} s_i^{(out)} s_j^{(in)} s_j^{(out)} s_i^{(in)}}{1 + z_{ij} s_i^{(out)} s_j^{(in)} + z_{ji} s_j^{(out)} s_i^{(in)} + r_{ij}^2 z_{ij} z_{ji} s_i^{(out)} s_j^{(in)} s_j^{(out)} s_i^{(in)}}, \tag{6}$$

$$P\left(A_{ij} = 1 \wedge A_{ji} = 0\right) = \frac{z_{ij} s_i^{(out)} s_j^{(in)}}{1 + z_{ij} s_i^{(out)} s_j^{(in)} + z_{ji} s_j^{(out)} s_i^{(in)} + r_{ij}^2 z_{ij} z_{ji} s_i^{(out)} s_j^{(in)} s_j^{(out)} s_i^{(in)}}, \tag{7}$$

$$P\left(A_{ij} = 0 \wedge A_{ji} = 0\right) = \frac{1}{1 + z_{ij} s_i^{(out)} s_j^{(in)} + z_{ji} s_j^{(out)} s_i^{(in)} + r_{ij}^2 z_{ij} z_{ji} s_i^{(out)} s_j^{(in)} s_j^{(out)} s_i^{(in)}}, \tag{8}$$

where $r \in \mathbb{R}_{>0}^{N\times N}$ with $r_{kl} = r_{lk}$ is a block specific parameter controlling for the number of reciprocal links. Again to simplify notation, r_{ij} denotes the r parameter of the corresponding block. Furthermore, since financial networks do not exhibit self-loops, we set $A_{ii} = 0$ for all $i = 1, \ldots, n$.

The parameter r comes from the term $\exp(-\lambda_r)$ of the discussed ERGM, with λ_r being the Lagrange multiplier of the constraint on the reciprocal links. Setting this Lagrange multiplier to zero $\lambda_r = 0$, or equivalently $r = 1$, and assuming pairwise independence for all links, results in the classical fitness model. This model has been studied in detail and it has been shown to yield good results, see for example Cimini et al. [16] and Gandy and Veraart [26]. Our model extends the classical fitness model by additionally incorporating the number of reciprocal links and therefore introducing a dependence structure between the dyads $\left(A_{ij}, A_{ji}\right)$. We decided to include the reciprocity in our model, since it has been shown to constitute an important network characteristic, that regarding most networks does not come as a natural consequence of the degree sequence, see for example Garlaschelli and Loffredo [27] and Bargigli et al. [8], and because it introduces only one additional parameter. As can be seen from the link probabilities, Eqs. (6) to (8), this setting correlates the number of links of a node to its weight, i.e. the higher the total incoming and outgoing weight of a node, the higher the number of incoming and outgoing links of a node. This is an essential characteristic that one would expect from financial networks, and which has been shown to hold in many empirical works, e.g. [45], [8].

Incorporating available information on the existence of certain links is straight forward. Let $a^* \in \{*, 0, 1\}^{n\times n}$, where $a_{ij} = *$ denotes an unknown link. The link probability matrix A is extended as follows,

$$A_{ij} = a_{ij}^*, \quad \forall a_{ij}^* \neq *. \tag{9}$$

In case only one of two reciprocal links is known, i.e. $a_{ij}^* \neq *$ and $a_{ji}^* = *$, the probability distribution of the unknown link is given by

$$P\left(A_{ji}=0|a^*_{ij}=0\right)=\frac{P\left(A_{ji}=0,A^*_{ij}=0\right)}{P\left(A_{ij}=0\right)}=\frac{1}{1+z_{ji}s_j^{(out)}s_i^{(in)}}, \tag{10}$$

$$P\left(A_{ji}=0|a^*_{ij}=1\right)=\frac{P\left(A_{ji}=0,A^*_{ij}=1\right)}{P\left(A_{ij}=1\right)}=\frac{z_{ij}s_i^{(out)}s_j^{(in)}}{z_{ij}s_i^{(out)}s_j^{(in)}+r_{ij}^2z_{ij}z_{ji}s_i^{(out)}s_j^{(in)}s_j^{(out)}s_i^{(in)}}, \tag{11}$$

$$P\left(A_{ji}=1|a^*_{ij}=0\right)=\frac{P\left(A_{ji}=1,A^*_{ij}=0\right)}{P\left(A_{ij}=0\right)}=\frac{z_{ji}s_j^{(out)}s_i^{(in)}}{1+z_{ji}s_j^{(out)}s_i^{(in)}}, \tag{12}$$

$$P\left(A_{ji}=1|a^*_{ij}=1\right)=\frac{P\left(A_{ji}=1,A^*_{ij}=1\right)}{P\left(A_{ij}=1\right)}=\frac{r_{ij}^2z_{ij}z_{ji}s_i^{(out)}s_j^{(in)}s_j^{(out)}s_i^{(in)}}{z_{ij}s_i^{(out)}s_j^{(in)}+r_{ij}^2z_{ij}z_{ji}s_i^{(out)}s_j^{(in)}s_j^{(out)}s_i^{(in)}}. \tag{13}$$

The unknown parameters z and r can be calibrated such that a desired number of links $L^{\rightarrow}$ and a desired number of reciprocal links $L^{\leftrightarrow}$ is met in expectation. The following three equations are used to calibrate the three parameters for each pair of transposed blocks $k, l = 1, \ldots, N$,

$$\mathbb{E}\left[\sum_{i\in C_k, j\in C_l} A_{ij}\right]=L^{\rightarrow}_{kl}, \qquad \text{(directed links)} \tag{14}$$

$$\mathbb{E}\left[\sum_{i\in C_l, j\in C_k} A_{ij}\right]=L^{\rightarrow}_{lk}, \qquad \text{(directed links)} \tag{15}$$

and

$$\mathbb{E}\left[\sum_{i\in C_k, j\in C_l} A_{ij}A_{ji}\right]=\mathbb{E}\left[\sum_{i\in C_l, j\in C_k} A_{ij}A_{ji}\right]=L^{\leftrightarrow}_{kl}. \qquad \text{(reciprocal links)} \tag{16}$$

There are many options to solve Eqs. (14) to (16), for example Matlab's nonlinear least-squares solver. For the blocks on the diagonal, i.e. for $k = l$ (representing domestic interbank markets), Eq. (14) and Eq. (15) are identical, hence there are only two equations to be solved. Once the two parameters are calibrated, sampling adjacency matrices, i.e. unweighted directed graphs, is easy and fast through bivariate Bernoulli trials.

If the desired number of links and reciprocal links are set to feasible numbers there always exists a solution, as the following theorem shows. Since the parameters z and r are independent for all pairs of submatrices $\left(A^{(kl)}, A^{(lk)}\right)$, it suffices to show the existence of a solution for one pair $\left(A^{(kl)}, A^{(lk)}\right)$.

Theorem 3.1 (Existence of a solution for the extended fitness model)
Consider four vectors $s^{(out,k)}, s^{(in,k)} \in \mathbb{R}^{n_k}_{>0}$, and $s^{(out,l)}, s^{(in,l)} \in \mathbb{R}^{n_l}_{>0}$. Let the random matrices $A^{(kl)} \in \{0,1\}^{n_k\times n_l}$ and $A^{(lk)} \in \{0,1\}^{n_l\times n_k}$ be defined by the probability function P as given by Eqs. (6) *to* (8)*. For any feasible number of*

(i) *reciprocal links $L^{\leftrightarrow}_{kl} \in [0, n_kn_l)$,*
(ii) *and links $\tilde{L}^{\rightarrow}_{kl} := L^{\rightarrow}_{kl} - L^{\leftrightarrow}_{kl}$ and $\tilde{L}^{\rightarrow}_{lk} := L^{\rightarrow}_{lk} - L^{\leftrightarrow}_{kl}$ with $\left(\tilde{L}^{\rightarrow}_{kl} + \tilde{L}^{\rightarrow}_{lk}\right) \in \left(0, n_kn_l - L^{\leftrightarrow}_{kl}\right)$,*

there exist $z_{kl}, z_{lk}, r_{kl} \in \mathbb{R}_{\geq 0}$, such that Eqs. (14) *to* (16) *are fulfilled.*

Proof of Theorem 3.1
For the proof see Appendix A.

The special case of $L^{\leftrightarrow}_{kl} = n_kn_l$ implies that $\tilde{L}^{\rightarrow}_{kl} = 0$ and $\tilde{L}^{\rightarrow}_{lk} = 0$, and hence, all links in the adjacency matrices $A^{(kl)}$ and $A^{(lk)}$ are set to 1. In the special case of $L^{\rightarrow}_{kl} = 0$, it follows that $z_{kl} = 0$ and $L^{\leftrightarrow}_{kl} = 0$, and we simply have to find a z_{kl} such that

$$\tilde{L}_{lk}^{\rightarrow} = \sum_{i \in C_k, j \in C_l} \frac{z_{kl} s_i^{(out)} s_j^{(in)}}{1 + z_{lk} s_j^{(out)} s_i^{(in)}}, \tag{17}$$

is satisfied. The existence of a solution to Eq. (17) follows from the intermediate value theorem. In the special case of $L_{kl}^{\rightarrow} = n_k n_l$, it follows that $L_{kl}^{\leftrightarrow} = L_{lk}^{\rightarrow}$. All links in $A^{(kl)}$ are set to 1 and for the random matrix $A^{(lk)}$, we consider the simplified problem of identifying z_{lk}, such that

$$L_{lk}^{\rightarrow} = \sum_{i \in C_k, j \in C_l} \frac{z_{kl} s_i^{(out)} s_j^{(in)}}{1 + z_{lk} s_j^{(out)} s_i^{(in)}}, \tag{18}$$

holds. Again, the existence of a solution to Eq. (18) follows from the intermediate value theorem.

To prove whether the solution of the extended fitness model is unique is non-trivial. However, we can show that the solution is unique w.r.t. the expected in- and out-degree sequences and the expected number of reciprocal links created by the solution.

Theorem 3.2 (Uniqueness of a solution for the extended fitness model)
A solution z_{kl}, z_{lk}, r_{kl} of the extended fitness model, as described in Theorem 3.1, yields the following particular sequences of expected in- and out-degrees,

$$d_j^{(in,kl)} = \sum_{i \in C_k} P\left(A_{ij}^{(kl)} = 1\right), \quad \text{for all } j \in C_l \tag{19}$$

$$d_i^{(out,kl)} = \sum_{j \in C_l} P\left(A_{ij}^{(kl)} = 1\right), \quad \text{for all } i \in C_k \tag{20}$$

$$d_j^{(in,lk)} = \sum_{i \in C_l} P\left(A_{ij}^{(lk)} = 1\right), \quad \text{for all } j \in C_k \tag{21}$$

$$d_i^{(out,lk)} = \sum_{j \in C_k} P\left(A_{ij}^{(lk)} = 1\right), \quad \text{for all } i \in C_l, \tag{22}$$

as well as the expected number of reciprocal links $L_{kl}^{\leftrightarrow}$. The solution z_{kl}, z_{lk}, r_{kl} is unique in the sense that it is the only parameter combination which generates the specific expected values $d_j^{(in,kl)}, d_i^{(out,kl)}, d_j^{(in,lk)}, d_i^{(out,lk)}$, and $L_{kl}^{\leftrightarrow}$.

Proof of Theorem 3.2
For the proof see Appendix A.

3.3. Allocation of weights via an ERGM

In a second step, we allocate weights to an adjacency matrix, sampled from the fitness model discussed in Section 3.2, through an exponential random graph model. The idea of ERGMs is to construct a probability distribution over a set of possible graphs by distributing the probability mass as uniformly as possible, while satisfying desired network statistics in expectation. For a detailed introduction to ERGMs and an overview over different existing classes of ERGMs, i.e. differences in the set of considered graphs and the constraints, see [42, 47, 28, 38, 32].

Let $a \in \{0,1\}^{n \times n}$ denote a realization of the random adjacency matrix A, as specified in the previous section. We define a set of possible weighted graphs $\mathcal{G}_a$ consistent with a, as the set of all graphs that assign weights in $\mathbb{N}_0$ to existing links of a and 0 weight to non-existing links of a:

$$\mathcal{G}_a = \left\{ w \in \mathbb{N}_0^{n \times n} \mid w_{ij} = 0, \forall a_{ij} = 0 \text{ and } w_{ij} \in \mathbb{N}_0, \forall a_{ij} = 1 \right\}. \tag{23}$$

Remark 3.1
We could further restrict the set of considered graphs, as the maximum weight that a link can carry is given

by the minimum of the corresponding row, column, and block weight, i.e.

$$\tilde{\mathcal{G}}_a = \left\{ w \in \mathbb{N}_0^{n\times n} \mid w_{ij} = 0, \forall a_{ij} = 0 \text{ and } w_{ij} \in \left\{1, 2, \ldots, \min\left\{s_i^{(out)}, s_j^{(in)}, s_{ij}^{(block)}\right\}\right\}, \forall a_{ij} = 1 \right\}. \tag{24}$$

The analytical derivation of this model works analogously to the one considering $\mathcal{G}_a$. However, the resulting expected link weights take a slightly more complex form, which renders parameter estimation more difficult. Since all expected weights, in the setting of $\mathcal{G}_a$, lie in the interval $\left(0, \min\left\{s_i^{(out)}, s_j^{(in)}, s_{ij}^{(block)}\right\}\right]$, in this paper we consider the simpler setting of $\mathcal{G}_a$.

Remark 3.2 (Partial knowledge of certain weights)
Incorporating available information on the weight of certain links is straight forward. Let $w^* \in \mathcal{W} := (\{*\} \cup \mathbb{N}_0)^{n\times n}$, where $w^*_{ij} = *$ denotes an unknown matrix element. In this case we simply consider the set of graphs

$$\mathcal{G}_{a,w^*} = \left\{ w \in \mathbb{N}_0^{n\times n} \mid w_{ij} = w^*_{ij}, \forall w^*_{ij} \neq * \text{ and } w_{ij} = 0, \forall a_{ij} = 0 \text{ and } w_{ij} \in \mathbb{N}_0, \forall a_{ij} = 1, w^*_{ij} = * \right\}. \tag{25}$$

The analytical derivation of this model works analogously to the one considering $\mathcal{G}_a$.

Further, let $\mathcal{P} := \{p : \mathcal{G}_a \to (0, 1)\}$ denote the set of all probability measures defined on $\mathcal{G}_a$. The most unbiased probability measure $p \in \mathcal{P}$, is the one with the minimum Kullback–Leibler divergence w.r.t. the uniform distribution, or equivalently with maximum Shannon entropy, and which fulfills the desired row sums, column sums, and block weights in expectation. This translates to the following constrained optimization problem,

$$\max_{p\in\mathcal{P}} - \sum_{w\in\mathcal{G}_a} p(w) \ln\left(p(w)\right) \tag{26}$$

subject to

$$\begin{aligned}
\sum_{w\in\mathcal{G}_a} p(w)\left(\sum_{j=1}^{n} w_{ij}\right) &= s_i^{(out)}, \quad \forall i = 1, \ldots, n, && \text{(assets)}\\
\sum_{w\in\mathcal{G}_a} p(w)\left(\sum_{i=1}^{n} w_{ij}\right) &= s_j^{(in)}, \quad \forall j = 1, \ldots, n, && \text{(liabilities)}\\
\sum_{w\in\mathcal{G}_a} p(w)\left(\sum_{i\in C_k, j\in C_l} w_{ij}\right) &= s_{kl}^{(block)}, \quad \forall k, l = 1, \ldots, N, && \text{(block weights)}\\
\sum_{w\in\mathcal{G}_a} p(w) &= 1.
\end{aligned} \tag{27}$$

This optimization problem can be solved with the method of Lagrange multipliers, by following the common steps in the context of ERGMs. The relevant calculations are summarized in the following. The graph Hamiltonian $H : \mathcal{G}_a \to \mathbb{R}$ is given by

$$H(w) = \sum_{i,j=1}^{n} \left(\theta_i^{(out)} + \theta_j^{(in)} + \theta_{ij}^{(block)}\right) w_{ij}, \tag{28}$$

where $\theta^{(out)}, \theta^{(in)} \in \mathbb{R}^n$, and $\theta^{(block)} \in \mathbb{R}^{N\times N}$ denote the corresponding Lagrange multipliers. To simplify the notation, let $\theta_{ij}^{(block)}$ denote the Lagrange multiplier of the corresponding block. Next, we derive the partition function Z. For further clarity we abbreviate $\theta_{ij} := \left(\theta_i^{(out)} + \theta_j^{(in)} + \theta_{ij}^{(block)}\right)$. W.l.o.g. let $a_{12} = 1$

$$\begin{aligned} Z &= \sum_{w\in\mathcal{G}_a} e^{-H(w)} = \sum_{w\in\mathcal{G}_a} \prod_{i\neq j} \exp\left(-\theta_{ij}w_{ij}\right) = \sum_{w\in\mathcal{G}_a} e^{-\theta_{12}w_{12}} \prod_{\substack{i\neq j\\(i,j)\notin\{(12)\}}} e^{-\theta_{ij}w_{ij}} \\ &= \left(\sum_{w\in\mathcal{G}_a|w_{12}=0} e^{-\theta_{12}w_{12}} \prod_{\substack{i\neq j\\(i,j)\notin\{(12)\}}} e^{-\theta_{ij}w_{ij}}\right) + \left(\sum_{w\in\mathcal{G}_a|w_{12}=1} e^{-\theta_{12}w_{12}} \prod_{\substack{i\neq j\\(i,j)\notin\{(12)\}}} e^{-\theta_{ij}w_{ij}}\right) + \dots \\ &= \left(\sum_{\tilde{w}_{12}=0}^{\infty} e^{-\theta_{12}\tilde{w}_{12}}\right) \underbrace{\left[\sum_{w\in\mathcal{G}_a|w_{12}=\tilde{w}_{12}} \prod_{\substack{i\neq j\\(i,j)\notin\{(12)\}}} e^{-\theta_{ij}w_{ij}}\right]}_{\text{constant for all } \tilde{w}_{12}} \\ &\overset{(\star)}{=} \prod_{(i,j)|a_{ij}=1} \left(\sum_{w_{ij}=0}^{\infty} e^{-\theta_{ij}w_{ij}}\right) = \prod_{(i,j)|a_{ij}=1} \frac{1}{1-e^{-\theta_{ij}}}, \qquad \text{by the geometric series,} \end{aligned} \tag{29}$$

where the same algebraic steps are applied to all elements in $(\star)$ as we applied exemplary to the first element w_{12}. Note that

$$e^{-\theta_{ij}} < 1 \tag{30}$$

has to hold for all (i, j) for which $a_{ij} = 1$, since otherwise the value of the partition function Z is infinity, which implies that p is not a solving probability measure.

From the general theory of ERGMs we known that taking partial derivatives of $F := -\ln(Z)$ w.r.t. the Lagrange multipliers yields the expected value of the corresponding constraint, see for example [24]. Thus, we get the following $\left(2n + N^2\right)$-dimensional system of equations, which can serve for calibrating the Lagrange multipliers,

$$\frac{\partial F}{\partial\theta_i^{(out)}} = \sum_{j|a_{ij}=1} \frac{\exp\left(-\theta_{ij}\right)}{1-\exp\left(-\theta_{ij}\right)} = s_i^{(out)}, \qquad \forall i = 1,\dots,n, \tag{31}$$

$$\frac{\partial F}{\partial\theta_j^{(in)}} = \sum_{i|a_{ij}=1} \frac{\exp\left(-\theta_{ij}\right)}{1-\exp\left(-\theta_{ij}\right)} = s_j^{(in)}, \qquad \forall j = 1,\dots,n, \tag{32}$$

$$\frac{\partial F}{\partial\theta_{kl}^{(block)}} = \sum_{i\in C_k, j\in C_l|a_{ij}=1} \frac{\exp\left(-\theta_{ij}\right)}{1-\exp\left(-\theta_{ij}\right)} = s_{kl}^{(block)}, \quad \forall k, l = 1,\dots,N. \tag{33}$$

Equivalently, taking the partial derivative F w.r.t. θ_{ij} yields the expected link weight, i.e.

$$\begin{aligned} \mathbb{E}\left[w_{ij} \mid a_{ij} = 1\right] &= \frac{\exp\left(-\theta_{ij}\right)}{1-\exp\left(-\theta_{ij}\right)}, \quad \forall i, j = 1,\dots,n, \\ \mathbb{E}\left[w_{ij} \mid a_{ij} = 0\right] &= 0, \qquad\qquad\qquad \forall i, j = 1,\dots,n. \end{aligned}$$

The question whether a solution for an ERGM exists is non-trivial and to the best of our knowledge still constitutes an open problem in the wider realm of the theory of ERMGs. Regarding the empirical analysis of the EU interbank market, conducted in Section 5, our algorithm for parameter estimation, see Section 4, was always able to quickly find a solution with minimal error. From the general theory of ERMGs, we know that if the set of solving distributions is non-empty, then all Lagrange parameters are unique up to possible equivalence classes.

Theorem 3.3 (Uniqueness of a solution for the ERGM)
If the set of probability measures $p \in \mathcal{P}$ that satisfy all constraints of Eq. (27) is non-empty, then the solving distribution function of the ERGM is unique up to certain equivalence classes. More precisely, the sum $\theta_{ij} = \left(\theta_i^{(out)} + \theta_j^{(in)} + \theta_{ij}^{(block)}\right)$ is unique for all $i, j = 1,\dots,n$ where $a_{ij} = 1$. Any set $\theta^{(out)}, \theta^{(in)}, \theta^{(block)}$

that matches the unique sums, defines the same solving probability measure and constitutes an equivalence class.

Proof of Theorem 3.3
For the proof see Appendix A.

4. Model calibration

Calibrating the Lagrange multipliers of the ERGM presented in Section 3.3 is demanding, since the system of equations is nonlinear, the number of parameters is (in most cases) very big, and because of the upper bound constraints of certain sums of the Lagrange multipliers (see Eq. (30)). For example, the reconstruction of the EU interbank network, conducted in Section 5, comprises $\left(2n + N^2\right) = \left(2 \cdot 3{,}469 + 29^2\right) = 7{,}779$ Lagrange multipliers. To solve this problem, we make use of the structural characteristics of the expected link weights and the system of equations.

We rewrite the problem in terms of $x_i^{(out)} := \exp\left(-\theta_i^{(out)}\right)$, $x_j^{(in)} := \exp\left(-\theta_j^{(in)}\right)$, and $x_{ij}^{(block)} := \exp\left(-\theta_{ij}^{(block)}\right)$, for all $i, j = 1, \ldots, n$. From the previous section we know that the matrix of expected link weights takes the following form, see Section 3.3, for $a \in \{0,1\}^{n\times n}$ a given adjacency matrix,

$$\mathbb{E}\left[w \mid a\right] = \left(\frac{x_i^{(out)} x_j^{(in)} x_{ij}^{(block)}}{1 - x_i^{(out)} x_j^{(in)} x_{ij}^{(block)}} a_{ij} \right)_{i,j=1,\ldots,n} . \tag{34}$$

The system of equations is essentially given by requiring the row sums, the column sums, and the block weights of $\mathbb{E}\left[w \mid a\right]$ to equal the desired weights $s^{(out)}, s^{(in)}$, and $s^{(block)}$, respectively. Moreover, the condition of Eq. (30) can be rewritten to $x_i^{(out)} x_j^{(in)} x_{ij}^{(block)} < 1$ for all (i, j) with $a_{ij} = 1$.

Next, we note that for given admissible parameters $x^{(in)} \in \mathbb{R}^n_{>0}$ and $x^{(block)} \in \mathbb{R}^{N\times N}_{>0}$, the equations of the row sums simplify to n independent, univariate non-linear functions. In addition, these functions are on the admissible support continuously differentiable and strictly monotonically increasing. Hence, this subproblem can easily be tackled for example by the univariate Newton's method. The same holds true when considering only the subset of column (block) parameters and column (block) equations. Therefore, we implement an iterative algorithm updating either the row, or the column, or the block parameters in each iteration w.r.t. the row, column, or block equations, respectively.

More precisely, in each iteration we compute three sums of the absolute errors consisting of the row constraints, the column constraints and the block constraints. The subset (row, column or block) with the highest error is selected for updating the respective subset of parameters by one step of the Newton's method. The Newton's method is scaled by a global *stepsize* parameter, that helps to control the impact on the disregarded equations, and that can be decreased as the algorithm moves towards a minimum. To ensure that the bounds of Eq. (30) are satisfied, we adjust a parameter update that would violate the lower (resp. upper) bound, by setting the concerned parameter to smallest (resp. largest) admissible value. The algorithm terminates, once an acceptable remaining error is reached.

As can be seen from Eq. (34), big desired weights $s^{(out)}, s^{(in)}$, and $s^{(block)}$, and thus big expected link weights, mean that the product of the parameters $x_i^{(out)} x_j^{(in)} x_{ij}^{(block)}$ gets pushed closer to 1. Hence, the bigger the desired weights $s^{(out)}, s^{(in)}$, and $s^{(block)}$, the more difficult the parameter calibration. Therefore, we consider the relative weights instead, i.e. all row, column, and block weights are divided by the total weight. Furthermore, as starting parameters we choose $x = s/(1 + s)$ which in our experiments works well, but any other starting values can be used likewise.

The pseudo-code of the algorithm is presented in Algorithm 1. Regarding the reconstruction of the EU interbank market, conducted in Section 5, the proposed algorithm is reasonably fast, compare Table 2.

Function `calibrate_ERGM`(*function:* `expectedWeights`, *vector:* $s^{(out)}$, *vector:* $s^{(in)}$, *matrix:* $s^{(block)}$, *matrix:* a)

for $i \leftarrow 1$ ***to*** n // set starting parameters
do
  $x_i^{(out)} \leftarrow s_i^{(out)} / \left(s_i^{(out)} + 1\right)$
  $x_i^{(in)} \leftarrow s_i^{(in)} / \left(s_i^{(in)} + 1\right)$
end
for $k \leftarrow 1$ ***to*** N **do**
  for $l \leftarrow 1$ ***to*** N **do**
    $x_{kl}^{(block)} \leftarrow s_{kl}^{(block)} / \left(\max\left\{s^{(block)}\right\}\right)$
  end
end
$w \leftarrow$ `expectedWeights`$(x^{(out)}, x^{(in)}, x^{(block)})$ // compute expected link weights

$errorRows \leftarrow \left(\sum |\, \texttt{rowSums}(w) - s^{(out)}\, |\right) / \left(\sum s^{(out)}\right)$ // get errors

$errorColumns \leftarrow \left(\sum |\, \texttt{colSums}(w) - s^{(in)}\, |\right) / \left(\sum s^{(in)}\right)$
$errorBlocks \leftarrow \left(\sum |\, \texttt{blockSums}(w) - s^{(block)}\, |\right) / \left(\sum s^{(block)}\right)$
$error \leftarrow \max\{errorRows, errorColumns, errorBlocks\}$ // choose subset with highest error

$errorAccept \leftarrow 1\%$ // set acceptable error threshold

$count \leftarrow 0$ // initialize parameters

$errorVec \leftarrow [errorRows, errorColumns, errorBlocks]$
$stepsize \leftarrow 0.1$
$stepAdj \leftarrow 100$

```
while error > errorAccept and count < 10^6 do
    switch max{errorRows, errorColumns, errorBlocks} do
        case errorRows                                   // update all x_i^(out)
            for i ← 1 to n do
                primeRowSum_i ← ∂/∂x_i^(out) ( Σ_{j=1}^n  x_i^(out) x_j^(in) x_ij^(block) / (1 − x_i^(out) x_j^(in) x_ij^(block)) 𝟙{a_ij=1} − s_i^(out) )
                x_i^(out) ← x_i^(out) − stepsize · ( rowSums(w)_i − s_i^(out) ) / primeRowSum_i
                if x_i^(out) > admissible support then
                    x_i^(out) ← max{admissible support}
                end
                else if x_i^(out) < admissible support then
                    x_i^(out) ← min{admissible support}
                end
            end
        end
        case errorColumns                                // update all x_i^(in)
            analogously
        end
        case errorBlocks                                 // update all x_i^(block)
            analogously
        end
    end
    w ← expectedWeights(x^(out), x^(in), x^(block))      // compute expected link weights
    errorRows ← ( Σ | rowSums(w) − s^(out) | ) / ( Σ s^(out) )    // get errors
    errorColumns ← ( Σ | colSums(w) − s^(in) | ) / ( Σ s^(in) )
    errorBlocks ← ( Σ | blockSums(w) − s^(block) | ) / ( Σ s^(block) )
    error ← max{errorRows, errorColumns, errorBlocks}    // choose subset with highest
     error
    errorVec ← [errorVec, [errorRows, errorColumns, errorBlocks]]
    count ← count + 1
    if length(errorVec) > stepAdj                        // adjust stepsize parameter
     then
        if mean(errorVec(end-stepAdj:end-stepAdj/2)) − mean(errorVec(end-stepAdj/2:end)) ≤ 1e − 4
         then
            stepsize ← stepsize/1.2
            errorVec ← min{errorVec}
            x^(in) ← best(x^(in))                        // restart at best solution found so far
            x^(out) ← best(x^(out))
            x^(block) ← best(x^(block))
        end
    end
end
return (x^(out), x^(in), x^(block))
```

Algorithm 1: Parameter calibration of the ERGM discussed in Section 3.3.

5. Empirical case study: Reconstructing the EU interbank network

In this section, we demonstrate how our model performs in reconstructing the EU interbank market. First, we discuss how the input variables can be estimated from publicly available data, and subsequently we present the simulation results. The simulated networks allow a detailed assessment of systemic risk, to which we make a first step in Section 6.

5.1. Data

The network characteristics that can be chosen in our model, compare Section 3, are

(i) interbank assets $s_i^{(out)}$ and liabilities $s_i^{(in)}$ for each bank i in the network;
(ii) the network density of each block, i.e. the number of links $L^{\rightarrow} \in \mathbb{N}^{N \times N}$;
(iii) the reciprocity of each block, i.e. the number of reciprocal links $L^{\leftrightarrow} \in \mathbb{N}^{N \times N}$ symmetric;
(iv) and the weight $s_{kl}^{(block)}$ of each block, $k, l = 1, \ldots, N$.

Even though the aggregated data of (ii) - (iv) do not reveal any individual bilateral lending information, these statistics are not explicitly available. Therefore, we show how this data can be approximated based on publicly available information. Total interbank assets and liabilities, on the other hand, are published in the banks' balance sheet. We obtain this data from the Bankscope (now Orbis Bank Focus) database of Bureau Van Dijk.

Roukny et al. [45] and Bargigli et al. [8] are granted access to real data from the German and Italian central bank and provide a detailed empirical analysis of the respective interbank markets. To the best of our knowledge, their works constitute the most extensive descriptions on the topology of financial networks of EU member states. Without further publicly available information, we propose to approximate the network densities within countries based on the information of the German and Italian interbank market. More precisely, for a country with $|C_j|$ banks we suggest a density equal to the average density found in the subgraphs of the German and Italian interbank market, consisting of the $|C_j|$ banks with the highest degree. This idea is motivated by the assumption that the difference in the number of banks in a country is mainly due to the number of small and local banks, while the need for a well connected core of big banks is universal. Hence, we assume that at least the density of the core of the interbank network is similar across countries. In case more information on interbank markets becomes available, the chosen density can easily be adjusted.

The density of the German and Italian interbank market, reduced to a number of best connected banks, can be derived via our earlier work [24] on the reconstruction of the unweighted German and Italian interbank market. Fig. 2 presents the average densities over 100 simulated German and Italian interbank networks, reduced to subgraphs of banks with the highest degree. Since the degree of a bank highly correlates with its weight, the subgraphs can also be interpreted to contain the biggest banks.

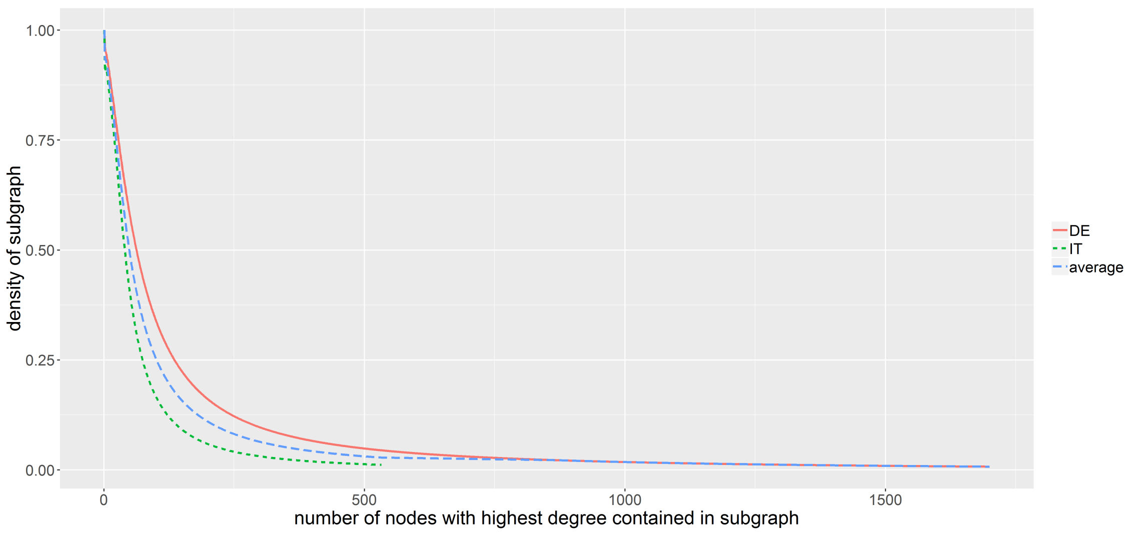

Figure 2: Average density over subgraphs of 100 German and 100 Italian simulated interbank networks, as well as the average over both countries. The size of the subgraphs is indicated on the x-Axis, and the selection is based on the (descending) degree of the banks.

To every country we assign a network density according to its number of banks and the average density over the German and Italian interbank networks, as presented by the dashed line in Fig. 2. A summary over all EU countries, their number of banks and allocated densities, is given in Table 1. The densities range from 93% for Malta, a country with only 5 banks, to 1% for Germany, a country with 1415 banks. It seems reasonable that countries comprising only a small number of banks are very well connected, while interbank networks of countries containing a large number of banks are rather sparse.

Table 1: Estimated network density for each country (data from 2016).

Country	AT	BE	BG	CY	CZ	DE	DK	EE	ES	FI	FR	GR	HR	HU
number of banks	527	33	14	22	19	1415	45	4	98	13	247	5	23	12
density	3%	65%	85%	77%	80%	1%	53%	93%	26%	86%	8%	93%	75%	87%

Country	IE	IT	LT	LU	LV	MT	NL	PL	PT	RO	SE	SI	SK	UK
number of banks	16	518	6	42	13	5	18	25	108	20	65	12	14	129
density	83%	3%	92%	56%	86%	93%	81%	73%	23%	79%	39%	87%	85%	19%

Next, we discuss the input factor of the block reciprocity. Degree reciprocity ρ_r is defined as the correlation coefficient between the symmetric entries of the adjacency matrix A of a directed graph, i.e. the tendency of nodes to form mutual links,

$$\rho_r := \frac{\sum_{i \neq j} \left(a_{ij} - \bar{a}\right)\left(a_{ji} - \bar{a}\right)}{\sum_{i \neq j} \left(a_{ij} - \bar{a}\right)^2}, \tag{35}$$

where $\bar{a}$ denotes the network density. The 'neutral' case $\rho_r = 0$ indicates that the network has exactly as many reciprocal links as expected in a random graph with the same number of vertices and links. Moreover, $\rho_r > 0$ (resp. $\rho_r < 0$) signifies that there are more (resp. less) reciprocal links than expected by chance. For a detailed discussion on reciprocity see Garlaschelli and Loffredo [27]. Roukny et al. [45] and Bargigli et al. [8] report a reciprocity of 0.31 for the German and 0.45 for the Italian interbank market. Without any further information on the reciprocity of other interbank markets, we decided to set the reciprocity of all blocks to the average of the two available values, i.e. to 0.38.

The estimation of the block weights is non-trivial, since there is no complete and consistent data set on cross border exposures publicly available. In an attempt to fill this gap and *"thus contributing to market discipline and financial stability in the EU"*[5] the European Banking Authority (EBA) conducts a transparency exercise since 2013. As part of this exercise, the EBA discloses interbank credit exposure of 131 (in 2016) European banks disaggregated on country level. We propose to use this data set to construct a prior distribution of credit exposure aggregated on country level. Subsequently, we derive the distribution of the block weights which is as close as possible to the prior distribution, i.e. the EBA data, while fulfilling the given marginals of total interbank assets and liabilities for each country, as given by the Bankscope database. As a distance function the Kullback–Leibler divergence can be used, which means we have to solve a simple maximum entropy problem. Furthermore, for the derivation of the block weights, we differentiate between cross-border active banks and domestic banks. As an approximation, we consider those banks as cross-border active which are marked as significant by the ECB[6] or which are classified as global systemically important banks (G-SIBs)[7]. The derivation of this distribution of the block weights is explained step by step in the following.

(1) For those countries for which the EBA data set includes at least one bank with a detailed country level distribution of its interbank credit exposures, we derive the relative distribution of credit exposure, aggregated over all listed banks in a country. The relative distribution is split to all EU countries, the rest of the world, and unallocated, which denotes the difference between total credit exposure and the sum over all listed country exposures.

[5] See `https://www.eba.europa.eu/-/eba-transparency-exercise`.

[6] See `https://www.bankingsupervision.europa.eu/banking/list/criteria/html/index.en.html`

[7] See `http://www.fsb.org/what-we-do/policy-development/systematically-important-financial-institutions-sifis/global-systemically-important-financial-institutions-g-sifis/`

(2) Countries for which we have a relative exposure distribution from the EBA and which comprise cross-border active banks: We derive block weights by distributing interbank assets of cross-border active banks according to the relative distribution from the EBA data set, and adding interbank assets of the domestic banks to the home country. For 2016 these countries are: AT, BE, CY, DE, ES, FI, FR, GR, IE, IT, LU, LV, MT, NL, PT, SE, SI, UK.

(3) Countries for which we have a relative exposure distribution from the EBA but are missing information on which banks are cross-border active: We approximate the relative amount of interbank assets of cross-border active banks by the mean over all countries with EBA and cross-border active information. This amount is then distributed according to the EBA data, while the corresponding amount of interbank assets of domestic banks is allocated to the home country. For 2016 these countries are: BG, DK, HU.

(4) Countries for which the cross-border active banks are known, but data of the EBA is missing: We approximate the amount of interbank assets of cross-border active banks that is allocated within the home country by the mean over all other domestic distributions of cross-border active banks that are allocated so far. The amount of interbank assets of domestic banks is also allocated to the home country. For 2016 these countries are: CZ, EE, LT, SK.

(5) Countries that are not comprised in the EBA data set and for which information on cross-border active banks is missing: A home bias is added by allocating the mean over all assigned home biases multiplied by total interbank assets of the respective countries. For 2016 these countries are: HR, PL, RO.

(6) Next, we compute how much of the countries interbank assets and liabilities, as given by Bankscope, are still unallocated. For countries for which we have already allocated a higher amount than available according to Bankscope, the value of the unallocated amount is set to zero.

(7) To distribute the unallocated interbank assets to the EU and to the rest of the world in a reasonable way, we allocate an amount of the sum of unallocated interbank assets to the rest of the world, that is proportional to the amount of weight that has been allocated to the rest of the world so far.

(8) The amount of interbank assets which is now still unallocated is spread over all EU blocks according to the unallocated marginals.

(9) In a last step we solve the optimization problem of minimizing the Kullback–Leibler divergence to the thus constructed prior distribution of block weights, subject to the marginal country constraints as given by Bankscope, i.e. total interbank assets and liabilities of each country have to be fulfilled.

The resulting distribution is presented in Fig. 3. For most countries, we can identify a clear home bias, visualized by the dark blue colors on the (anti-) diagonal. Furthermore, some countries allocate a substantial amount of their interbank assets to France, the rest of the world, Italy, Spain, UK, and Germany. Regarding interbank liabilities, a substantial amount comes from countries outside of the EU, as well as France and Italy.

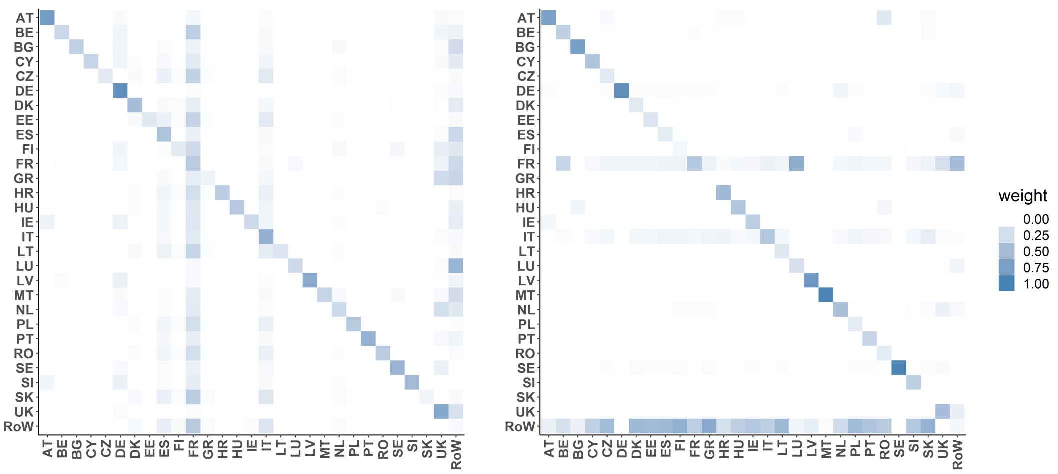

Figure 3: Distribution of interbank assets and liabilities, based on the EBA transparency exercise of 2016. The plot on the left shows how each country distributes its interbank assets, i.e. each row sums up to one. The plot on the right shows where the interbank liabilities of each country come from, i.e. each column sums up to one. ‘RoW’ denotes the ‘Rest of the World’.

The last input factor that we need to discuss is the density of cross-border blocks. Since at this point, we have already derived the density of each country and the block weights, we can compute the average weight per link within each country. Without further information on cross-border interbank markets, we propose to take the minimum weight per link of two countries as a proxy for the weight per link of the cross-border block between both countries. This means the number of links in the cross-border matrix of countries k and l is approximated by

$$L_{kl}^{\rightarrow} = \left(\min \left\{ \frac{s_{kk}^{(block)}}{L_{kk}^{\rightarrow}}, \frac{s_{ll}^{(block)}}{L_{ll}^{\rightarrow}} \right\} \right)^{-1} \cdot s_{kl}^{(block)}. \tag{36}$$

This section illustrated one approach to estimate the model input factors based on scarce publicly available information. Moreover, these factors only serve for calibration and do not impact the methodological part of the model. Also, in case further aggregated data on financial networks, such as the density, degree distribution, block weights, or reciprocity become available in the future, our model can easily incorporate this information. Actually, policy-makers might already have access to some additional, not publicly available data, that they can use to calibrate the model more accurately.

5.2. *Simulation results*

The model derived in Section 4 together with the data discussed in Section 5.1 allows us to reconstruct the EU interbank network. In the following, the results are presented.

The case study is based on data of 2016, for which Bankscope lists 3,468 unconsolidated EU banks with positive interbank assets and liabilities. Adding a Rest-of-the-World node leads to a network of 3,469 nodes and 29 regions (28 EU countries + Rest-of-the-World), i.e. $29^2 = 841$ blocks. There are two sources of errors that should be differentiated. First, an adjacency matrix might be drawn that has no links in some rows, columns, and blocks, and hence no weight can be allocated. Second, the weight allocation found by Algorithm 1 yields a remaining error. Table 2 summarizes the runtime and the error of both parts of the model. The relative error of the row sums (column sums/ block weights) refers to the sum of absolute errors over all rows (columns/ blocks) divided by the sum of all row (column/ block) weights.

Table 2: Runtime and error of the Fitness model and the ERGM, w.r.t. 100 simulated interbank networks (including the Rest-of-the-World node) and with an acceptable error threshold of 1% in Algorithm 1.

	Fitness Model adjacency matrix		ERGM weight allocation	
	mean	std	mean	std
runtime	36 seconds	NA	2.5 min/ network	NA
relative error row sums	3.86e-04	3.40e-05	9.81e-03	1.42e-04
relative error column sums	3.22e-04	3.05e-05	9.83e-03	1.34e-04
relative error block weights	1.00e-02	1.40e-05	9.85e-03	1.10e-04

To gain some insight into the topology of the simulated networks, Table 3 reports the most prominent network statistics. Unfortunately, we do not have access to data on the actual EU interbank market and hence, cannot conduct a detailed assessment of the goodness-of-fit. However, our model seems to successfully reproduce some commonly reported characteristics of financial networks, such as sparsity, a positive reciprocity, disassortativity, and short paths.

Table 3: Mean, standard deviation, and 95% confidence interval of different network statistics, w.r.t. 100 simulated networks (excluding the Rest-of-the-World node).

	mean	std	95% confidence interval
total number of links	69,451	223	[69,408; 69,495]
number of reciprocal links	26,995	163	[26,964; 27,027]
in-degree assortativity	-0.23	0.0026	[-0.23; -0.23]
out-degree assortativity	-0.19	0.0017	[-0.19; -0.19]
directed clustering coefficient	0.66	0.0036	[0.66; 0.66]
undirected clustering coefficient	0.72	0.0032	[0.72; 0.72]
shortest directed path	2.92	0.0079	[2.92; 2.92]
shortest undirected path	2.95	0.0092	[2.94; 2.95]
number of isolated nodes	81	8	[80; 83]
largest strongly connected component	2,828	17	[2,824; 2,831]
largest weakly connected component	3,387	8	[3,385; 3,388]

Since the simulated networks serve as basis for an assessment of systemic risk, the network similarity within the drawn sample is also of interest. If the location of the links and their weight does not change much across the sample, systemic risk results will be very stable as well. With increasing variation in the sampled networks, however, we expect an increasing variance and uncertainty in the quantification of systemic risk. Therefore, we now analyze the similarity of the sampled adjacency matrices and the allocated weights. The similarity between two realizations a and $\tilde{a}$ of the link probability matrix $A \sim Bin\left(1, (p_{ij}, p_{ji})\right)^{n\times n}$ can be derived analytically. The expected number of links that exist in both adjacency matrices is given by

$$\begin{aligned}
&\mathbb{E}\left[\sum_{i\neq j} \mathbb{1}_{\{a_{ij}=1\wedge\tilde{a}_{ij}=1\}}\right] \\
&= \mathbb{E}\Bigg[\sum_{i<j} \mathbb{1}_{\{a_{ij}=1\wedge a_{ji}=0\wedge\tilde{a}_{ij}=1\wedge\tilde{a}_{ji}=0\}} + \mathbb{1}_{\{a_{ij}=1\wedge a_{ji}=0\wedge\tilde{a}_{ij}=1\wedge\tilde{a}_{ji}=1\}} \\
&\qquad + \mathbb{1}_{\{a_{ij}=0\wedge a_{ji}=1\wedge\tilde{a}_{ij}=0\wedge\tilde{a}_{ji}=1\}} + \mathbb{1}_{\{a_{ij}=0\wedge a_{ji}=1\wedge\tilde{a}_{ij}=1\wedge\tilde{a}_{ji}=1\}} \\
&\qquad + 2\mathbb{1}_{\{a_{ij}=1\wedge\tilde{a}_{ij}=1\wedge a_{ji}=1\wedge\tilde{a}_{ji}=1\}} + \mathbb{1}_{\{a_{ij}=1\wedge\tilde{a}_{ij}=1\wedge a_{ji}=1\wedge\tilde{a}_{ji}=0\}} + \mathbb{1}_{\{a_{ij}=1\wedge\tilde{a}_{ij}=1\wedge a_{ji}=0\wedge\tilde{a}_{ji}=1\}}\Bigg] \\
&= \sum_{i<j} \mathbb{P}\left(a_{ij}=1\wedge a_{ji}=0\wedge\tilde{a}_{ij}=1\wedge\tilde{a}_{ji}=0\right) + \ldots + 2\mathbb{P}\left(a_{ij}=1\wedge\tilde{a}_{ij}=1\wedge a_{ji}=1\wedge\tilde{a}_{ji}=1\right) \\
&= \sum_{i<j} p_{ij}^{(1,0)}\left(p_{ij}^{(1,0)}+p_{ij}^{(1,1)}\right) + p_{ij}^{(0,1)}\left(p_{ij}^{(0,1)}+p_{ij}^{(1,1)}\right) + p_{ij}^{(1,1)}\left(2p_{ij}^{(1,1)}+p_{ij}^{(1,0)}+p_{ij}^{(0,1)}\right).
\end{aligned} \tag{37}$$

The expected numbers of links that differs and that is absent in a and $\tilde{a}$ can be computed analogously. Table 4 summarizes the expected similarity and dissimilarity between two sampled adjacency matrices of the reconstructed EU interbank market. In expectation, almost half of the sampled links in the network will be identical in both realizations, and half of the sampled links will change location. Regarding the sampled zeros in the adjacency matrices, i.e. non-existing links, on average 99.7% of the zeros will be identical in two realizations.

Table 4: Expected similarities and dissimilarities in the sampled adjacency matrices modeling the EU interbank market (excluding the Rest-of-the-World node) if two independent simulation runs are drawn.

fraction of existing links that is identical in two runs	fraction of existing links that differs in two runs	fraction of absent links that is identical in two runs
$\frac{\mathbb{E}\left[\sum_{i,j}\mathbb{1}_{\{a_{ij}=1\wedge\tilde{a}_{ij}=1\}}\right]}{\mathbb{E}\left[\sum_{i,j}a_{ij}\right]} = 48.81\%$	$\frac{\mathbb{E}\left[\sum_{i,j}\mathbb{1}_{\{a_{ij}=1\wedge\tilde{a}_{ij}=0\}}\right]}{\mathbb{E}\left[\sum_{i,j}a_{ij}\right]} = 51.19\%$	$\frac{\mathbb{E}\left[\sum_{i,j}\mathbb{1}_{\{a_{ij}=0\wedge\tilde{a}_{ij}=0\}}\right]}{\mathbb{E}\left[\sum_{i,j}1-a_{ij}\right]} = 99.70\%$

Next, we analyze the similarity between the allocated weights. Since the parameters of the ERGM are recalibrated for every realization of the adjacency matrix, the similarity between the weights cannot be derived analytically. Therefore, we compute two empirical similarity measures: the relative difference and the cosine similarity. Let w and $\tilde{w}$ denote two realizations of the EU interbank market. The relative difference between w and $\tilde{w}$ is given by

$$\frac{\sum_{ij}|w_{ij} - \tilde{w}_{ij}|}{\sum_{ij} w_{ij} + \sum_{ij} \tilde{w}_{ij}}.$$

Comparing all 100 simulated networks pairwise yields an average relative difference of 0.18 and a standard deviation of 0.002. The cosine similarity is defined as

$$\frac{\sum_{i,j} w_{ij}\tilde{w}_{ij}}{\sqrt{\sum_{i,j} w_{ij}^2}\sqrt{\sum_{i,j} \tilde{w}_{ij}^2}}. \tag{38}$$

Interpreting both networks as n^2-dimensional vectors, the cosine similarity gives the cosine of the angle between the two vectors. Since all weights are non-negative, the cosine similarity is bounded by $[0, 1]$ with 1 (resp. 0) signifying the strongest (resp. least) possible similarity. Comparing the sampled networks pairwise, gives an average cosine similarity of 0.98 and a standard deviation of 0.002.

The high cosine similarity together with the high number of changing links and a substantial difference in weight allocation, suggest that links with high weights, connecting big banks, stay quite constant over the set of sampled networks, while links with small weights, involving at least one small bank, vary notably (in existence and weight). This assumption can be verified by plotting the elements of sampled network matrices against each other, see Fig. 4.

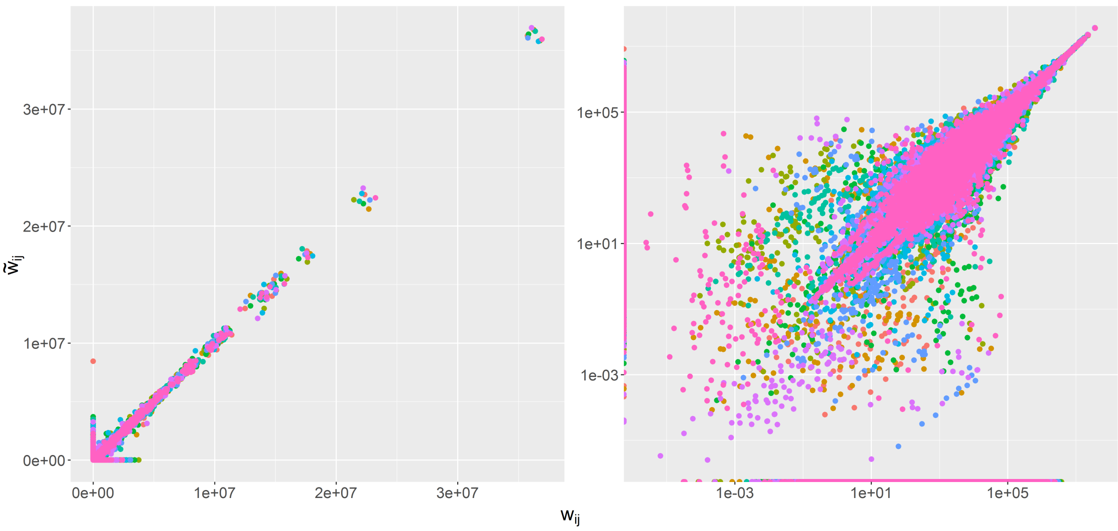

Figure 4: Scatterplot of link weights w_{ij} and $\tilde{w}_{ij}$, comparing 10 simulated networks pairwise (i.e. network 1 vs. network 2, network 2 vs. network 3, ..., network 9 vs. network 10). Links that do not exist in neither of the two respectively considered networks are omitted. The figure on the right is in log-log scale.

6. Assessing systemic risk in the EU interbank market

Our network reconstruction model enables the application of various contagion mechanisms and systemic risk measures to realistic, international financial networks. To demonstrate this, we conduct a systemic risk analysis on a sample of reconstructed EU interbank networks. The following results are computed by the 'FINEXUS Leverage Network Framework for Stress-testing' software of Gabriele Visentin, Marco D'Errico, and Stefano Battiston [9, 52], which integrates five of the most popular financial contagion models, namely: the 'clearing vector' by Eisenberg and Noe (EN) [22], the 'extended clearing vector' incorporating default costs by Rogers and Veraart (RV) [43], the 'default cascades model' (DC) by Battiston et al. [10], the 'acyclic DebtRank' (aDR) by Battiston et al. [11], and the 'cyclic DebtRank' (cDR) by Battiston et al. [7].

Furthermore, following [9, 52] we differentiate between two risk dimensions. First, there is the risk that a bank under stress triggers waves of contagious losses throughout the entire system. Second, there is the risk that a bank is vulnerable to other banks in the network being under stress. More precisely, we distinguish:

- **Global Vulnerability** = relative loss in equity that a shock scenario causes to the entire system;
- **Individual Vulnerability** = relative loss in equity that a bank suffers from a shock scenario.

To keep individual vulnerability comparable across banks, in the following we consider instead the absolute loss in equity suffered by each bank.

There are many interesting questions regarding systemic risk that can now be analyzed. Here, we focus on the following four aspects. First, we give a general overview over the network fragility for various shock sizes and according to the different contagion models, see Section 6.1. Subsequently, Section 6.2 describes the correlation of node characteristics and systemic risk. In Section 6.3 we compare the official list of G-SIBs in the EU, provided by the Basel Committee on Banking Supervision, with our results. Last, in Section 6.4, we analyze the question how network density, an indicator of diversification in interbank lending, affects financial stability and compare our findings with the literature.

Throughout this section, a recovery rate of 40% is used for all banks.[8] The contagion model of Rogers and Veraart (RV) additionally considers a recovery rate for external assets, which is fixed to 50%, the default value of the 'FINEXUS Leverage Network Framework for Stress-testing' software. Moreover, 'first Round' effects refer to initial losses, caused solely by external shocks on the banks, disregarding propagation. 'Second Round' effects, computed by the different contagion models, report additional losses due to contagion, excluding first round losses.

6.1. Systemic risk for different shock sizes

We start the assessment of systemic risk by shocking all banks equally with various shock sizes and by propagating the shocks according to five different contagion models. Figures 5 and 6 present the resulting loss in equity and the fraction of defaulted banks. Comparing our results to those of Visentin et al. [52], who analyze systemic risk in reconstructed networks of the 50 largest banks in the EU, we find that our networks are more stable, but the structure of the curves is very similar. Interestingly however, we observe a slightly different partial ordering for the global vulnerability H:

$$H^{\text{EN}} \leq H^{\text{RV}} \leq H^{\text{DC}} \leq H^{\text{aDR}} \leq H^{\text{cDR}}. \tag{39}$$

In all simulations analyzed by Visentin et al. [52], the authors find the following partial ordering:

$$H^{\text{EN}} \leq H^{\text{DC}} \leq H^{\text{RV}} \leq H^{\text{aDR}} \leq H^{\text{cDR}}. \tag{40}$$

Whether the DC or the RV model yields higher global losses depends on the shock size and on the recovery rates. In both the DC and the RV model banks spread losses only in case of their default. Within the DC model, a defaulted bank triggers distress to its interbank creditors proportionally to the nominal liabilities times one minus the recovery rate, as soon as the losses suffered reach the bank's equity. In the RV model, in contrast, only the amount of a bank's obligations (external plus interbank liabilities) that exceeds its assets (external plus interbank assets) is spread proportionally to all creditors (external plus interbank creditors) times one minus the recovery rate. Hence, if a bank suffers a shock equal to the size of its equity, in the DC model it will propagate the maximum loss that it can spread, while in the RV model, it will simply absorb this shock and no propagation takes place. Moreover, in the RV model part of the distress flows out of the interbank network, since losses are also propagated to external creditors (via external liabilities). However, in the RV model a bank can suffer shocks higher than its equity. Therefore, with increasing shock sizes the losses spreading through the RV model will increase. The DC model, on the other hand, saturates at shock levels equal to the size of the banks' equity. Another important parameter that determines losses in the RV model is the recovery rate on external assets (which is set to 50% in all considered examples).[9]

[8] See, for example, `www.cdsmodel.com` and [3].

[9] For more details on the contagion models see e.g. Visentin et al. [52] and references therein.

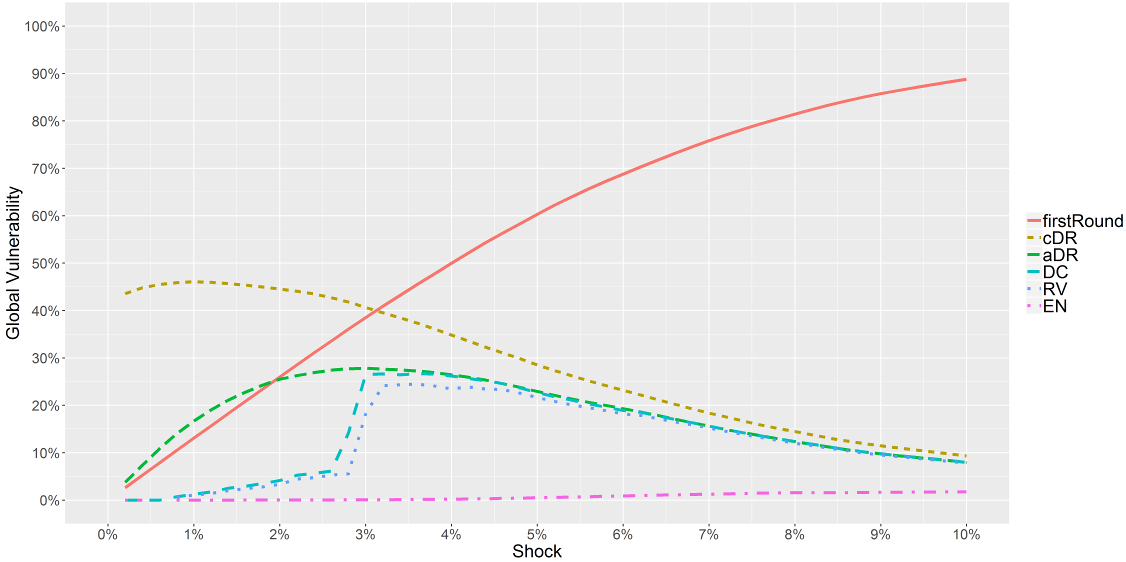

Figure 5: Global vulnerability caused by shocking all banks equally with various shock sizes and for different contagion models. Reported values are averages over 100 simulated networks (excluding the Rest-of-the-World node).

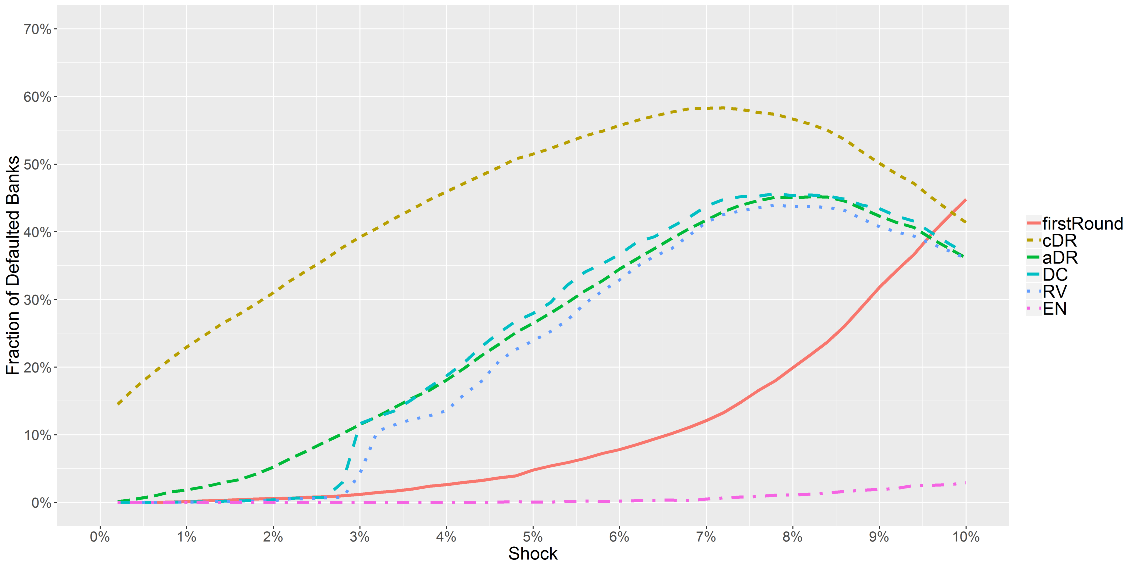

Figure 6: Fraction of defaulted banks caused by shocking all banks equally with various shock sizes and for different contagion models. Reported values are averages over 100 simulated networks (excluding the Rest-of-the-World node).

6.2. Correlation of node characteristics and systemic risk

In this paragraph we investigate:

1) Which network statistics make a node systemically important, in the sense that its default causes a severe shock on the entire banking network?
2) Which network statistics make a node vulnerable towards the default of other banks in the system?

We analyze both questions empirically in our set of reconstructed EU interbank networks, by letting one bank default at a time and computing the impact on the entire system as well as towards each of the other banks individually. As network statistics we consider the nodes' degree and strength and their centrality w.r.t. the (un-) directed and (un-) weighted network. In the framework of DC, aDR, and cDR a bank defaults as soon as the loss suffered reaches the value of its equity. At this point the defaulted bank triggers the maximum loss spread that it can cause (which equals the sum of its outstanding interbank liabilities multiplied by one minus its recovery rate). Even if the loss suffered exceeds the bank's equity level, the triggered loss spread does not increase further. Therefore, in the following, we initiate a bank's default by a shock on its external assets in the size of its equity. However, the EN and RV model assume that losses up to the size of a bank's equity can be absorbed by the bank and only losses exceeding the equity level are spread to the system. Hence, shocking a single bank by a loss equal to the size of its equity causes only the respective bank to default and no further losses occur. So, in this setting, global vulnerability in the EN and RV model equals simply the relative value of the defaulted bank's equity w.r.t. the total equity in the network. Analogously, individual vulnerability (i.e. losses suffered by a bank upon the default of another bank) equals zero in the EN and RV model.

Table 5 reports the rank correlation, measured by Kendall's tau, between different network statistics of the nodes and the relative loss in equity on the entire system caused by the nodes' default. Since shocks propagate backwards, from a node to its creditors, we can observe a high correlation between a node's number of incoming links as well as the weight carried by these links and global vulnerability. Regarding the centrality measures, interestingly closeness centrality seems to be the most relevant. Closeness centrality is defined as the inverse of the average distance from a node to the other nodes in the network. Hence, the shorter the paths between a bank and the other banks in the network, the higher its systemic impact, which is exactly what one would expect.

The correlation of nodes characteristics and individual vulnerability is presented in Table 6. Overall, we observe a high positive correlation between the number of outgoing links as well as their carried weight and individual vulnerability. Again, in most cases, closeness centrality turns out to be the most relevant centrality measure.

Table 5: Kendall's tau for different node characteristics and global vulnerability caused by the default of the respective node. Values of the EN and RV model essentially report the correlation with the banks' equity, since in the considered shock setting no propagation is triggered. All values are statistically highly significant with p-values smaller than 1e-200.

	EN	RV	DC	aDR	cDR
in-degree	0.57	0.57	0.65	0.63	0.68
in-strength	0.61	0.61	0.72	0.84	0.79
closeness undirected unweighted	0.61	0.61	0.67	0.72	0.62
in-closeness unweighted	0.58	0.58	0.67	0.75	0.72
closeness undirected weighted	0.67	0.67	0.75	0.79	0.68
in-closeness weighted	0.58	0.58	0.69	0.85	0.77
betweenness undirected unweighted	0.56	0.56	0.59	0.52	0.51
betweenness directed unweighted	0.55	0.55	0.58	0.53	0.54
betweenness undirected weighted	0.52	0.52	0.51	0.50	0.50
betweenness directed weighted	0.48	0.48	0.54	0.54	0.49
eigenvector centrality undirected unweighted	0.60	0.60	0.65	0.69	0.55
eigenvector centrality undirected weighted	0.45	0.45	0.51	0.61	0.45

Table 6: Kendall's tau for different node characteristics and individual vulnerability suffered by the respective node and caused by the default of other nodes. Values for the EN and RV model are not available, since in the considered shock setting no propagation is triggered. All values are statistically highly significant with p-values smaller than 1e-14.

	EN	RV	DC	aDR	cDR
out-degree	NA	NA	0.68	0.63	0.57
out-strength	NA	NA	0.95	0.89	0.82
closeness undirected unweighted	NA	NA	0.55	0.58	0.60
out-closeness unweighted	NA	NA	0.72	0.74	0.76
closeness undirected weighted	NA	NA	0.62	0.65	0.65
out-closeness weighted	NA	NA	0.85	0.83	0.78
betweenness undirected unweighted	NA	NA	0.59	0.56	0.53
betweenness directed unweighted	NA	NA	0.61	0.58	0.55
betweenness undirected weighted	NA	NA	0.50	0.51	0.51
betweenness directed weighted	NA	NA	0.55	0.55	0.55
eigenvector centrality undirected unweighted	NA	NA	0.46	0.49	0.49
eigenvector centrality undirected weighted	NA	NA	0.34	0.38	0.40

6.3. Global Systemically Important Banks (G-SIBs)

One methodology for identifying global systemically important banks (G-SIBs) was proposed by the Basel Committee on Banking Supervision (BCBS). It is essentially a weighted sum over a number of normalized financial positions. The BCBS states: *"The Committee is of the view that global systemic importance should be measured in terms of the impact that a bank's failure can have on the global financial system and wider economy, rather than the risk that a failure could occur. This can be thought of as a global, system-wide, loss-given-default (LGD) concept rather than a probability of default (PD) concept."*, (see `https://www.bis.org/publ/bcbs255.pdf`).

As our model allows to directly simulate the failure of a single bank and, hence, to compute the LGD in the interbank market, naturally the question arises whether the ranking in terms of global vulnerability is aligned to the one derived by the BCBS methodology. Differences in the two approaches that should be kept in mind are listed in Table 7.

Table 7: Differences in the assessment of G-SIBs.

	BCBS	Model presented in Sections 3 to 5
coverage	worldwide	EU
aggregation level of banks	consolidated	unconsolidated
LGD w.r.t.	global economy	interbank market

Figure 7 compares the scores of the BCBS against global vulnerability caused by the single default of each bank. The default of a bank is again initiated by a shock on external assets in the size of the bank's equity. Hence, in the EN and RV model global vulnerability equals the relative value of the bank's equity w.r.t. the total equity in the network. We observe that the ranking of the banks differs substantially across the contagion models. A low but significant rank correlation between the BCBS methodology and global vulnerability can only be identified for the EN and the RV model, see Table 8. Thus, the BCBS ranking is more aligned with the equity of the banks, than with the systemic risk computed by the DC, aDR, and cDR in our reconstructed EU interbank networks.

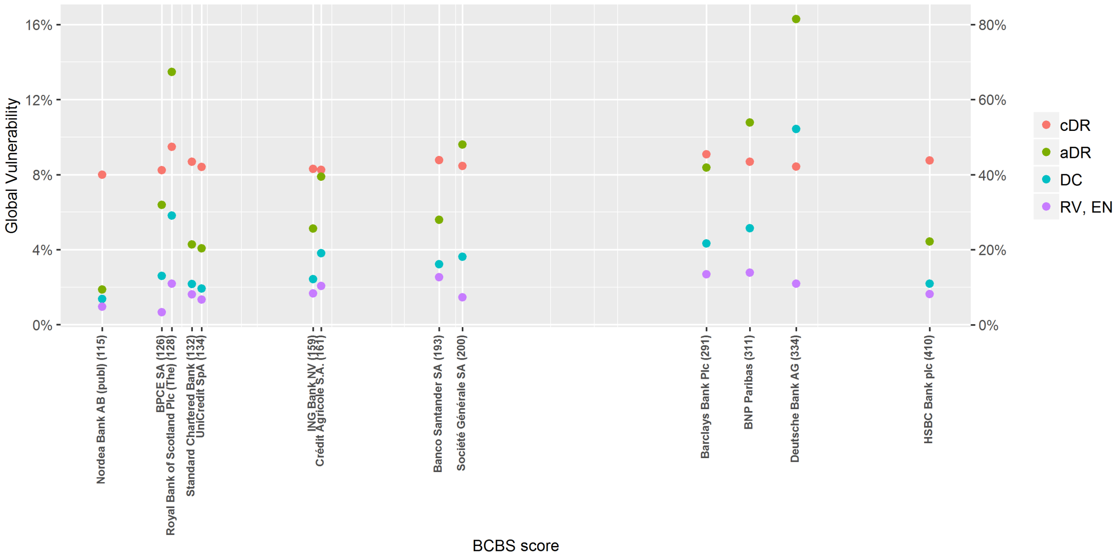

Figure 7: Comparison of G-SIBs in the EU as classified by the BCBS' methodology (scores on the x-axis in log scale) and global vulnerability (on the y-axis). The secondary y-axis (right) refers to global vulnerability computed by the cDR. Global vulnerability values are averages over 100 simulated networks (excluding the Rest-of-the-World node). Note that the y-axis denotes the relative loss in equity while the scale of the x-axis is difficult to interpret.

Table 8: Kendall's tau of the ranking of the G-SIBs in the EU between the BCBS' classification and global vulnerability. Significance at the level of 5% is marked by '*'.

	EN, RV	DC	aDR	cDR
Kendall's tau	0.46*	0.41	0.38	0.28
p-value	0.03	0.06	0.08	0.20

In addition to the computation of a LGD, our model also allows for a detailed analysis of the consequences of one of the G-SIBs being under stress. For example, we can simulate a shock of arbitrary size to a G-SIBs and compute the resulting network-wide loss. Figure 8 illustrates these shock scenarios exemplary for the Deutsche Bank AG and w.r.t. all five contagion models.[10] The point on the x-axis at which a function turns into a constant marks the shock size at which the bank defaults, i.e. the point at which the absolute value of the shock equals the bank's equity. In the DC, aDR, and cDR this triggers the maximum loss spread that a bank can propagate (which equals the total amount of its outstanding interbank liabilities adjusted by the recovery rate). We observe that the amount of total losses depends heavily on the chosen contagion model.

[10]Equivalent plots for the other G-SIBs in the EU are included in Fig. 10.

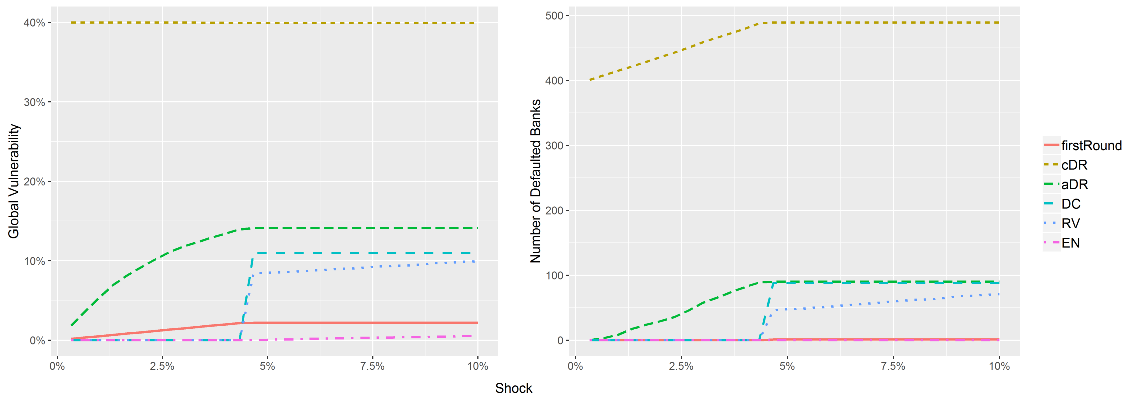

Figure 8: Global vulnerability (left) and number of defaults (right) caused by shocking the Deutsche Bank AG with shock sizes ranging from 1% to 10% of external assets, computed by the contagion models: EN, RV, DC, aDR, and cDR. Reported values are averages over 100 simulated networks (excluding the Rest-of-the-World node).

In summary, our model enables a detailed systemic risk analysis. The BCBS's methodology, on the other hand, allows for a fast calculation and incorporates indicators covering the global economy. Table 9 gives an overview over advantages and disadvantages of both methodologies.

Table 9: Advantages and disadvantages of the BCBS's methodology and our model

	BCBS methodology	Model presented in Sections 3 to 5
Advantages	• fast calculation • covers the global economy	• resulting score has a monetary interpretation • analysis of arbitrary shock sizes (< default) is possible • analysis of simultaneously shocking several banks is possible • distribution of shock impact can be estimated • new regulations can be tested • impact of network statistics on systemic risk can be analyzed
Disadvantages	• scale of scores has no interpretation	• some input parameters are not known explicitly, i.e. need to be estimated • data availability limits the scope of the model, i.e. determines which countries can be included • systemic risk values are not deterministic across different simulated networks, but seem to have a very low standard deviation • covers only the EU interbank market

6.4. *Network density and stability*

Another question is how the network density, an indicator of diversification in interbank lending, influences financial stability. This aspect has already been analyzed in several papers. Recently, Roncoroni et at. (2018) [44] confirmed earlier results of Acemoglu et al. (2015) [1] that densely connected networks are more stable regarding small shocks, but more fragile regarding big shocks. [1] base their analysis on artificial networks and focus mostly on regular networks (= total claims and liabilities of all banks are equal). [44], on the other hand, analyze a unique dataset of the European Central Bank, consisting of 26 large EU banks.

Are these results confirmed within our sample of reconstructed EU interbank networks, comprising 3,468 banks?

To answer this question, we construct a second network ensemble, where the density of each block was increased to $d^{(new)} = d^{(old)} + (1 - d^{(old)})/2$. The density matrix is presented in form of a heatmap in Fig. 9.

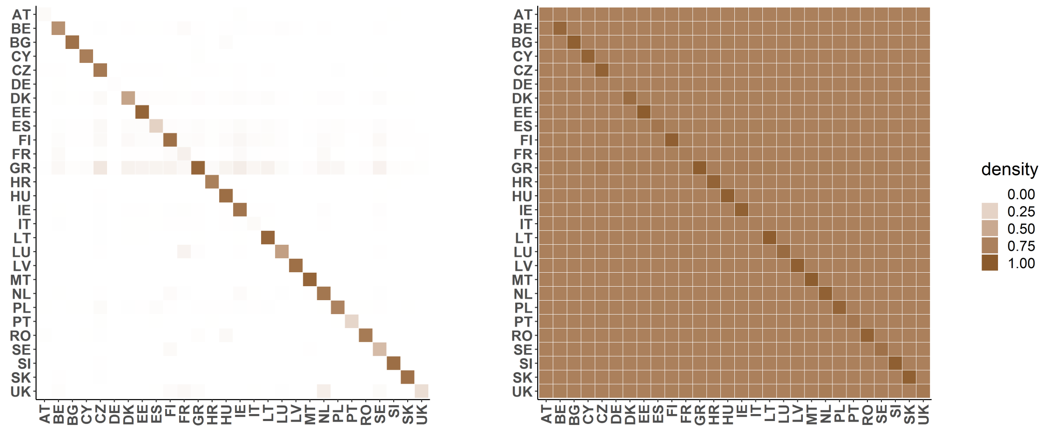

Figure 9: Heatmap of original densities (left) and increased densities (right).

First, we analyze the effect of the increased network density on the G-SIBs. Figure 10 presents the results of shocking the G-SIBs banks separately in the more densely connected networks in comparison to the originally sparse networks, computed by the EN, RV, DC, aDR, and cDR contagion model. In almost all considered cases, global vulnerability and the number of defaulting banks is smaller in the densely connected networks. The magnitude of the difference depends heavily on the applied contagion model.

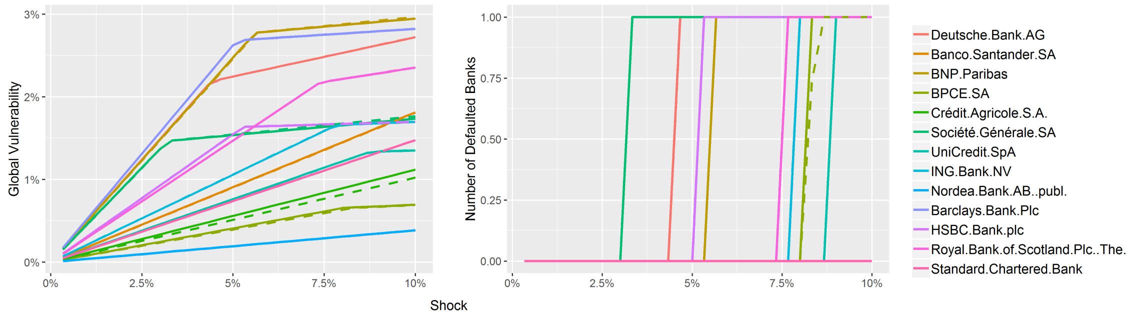

(a) EN

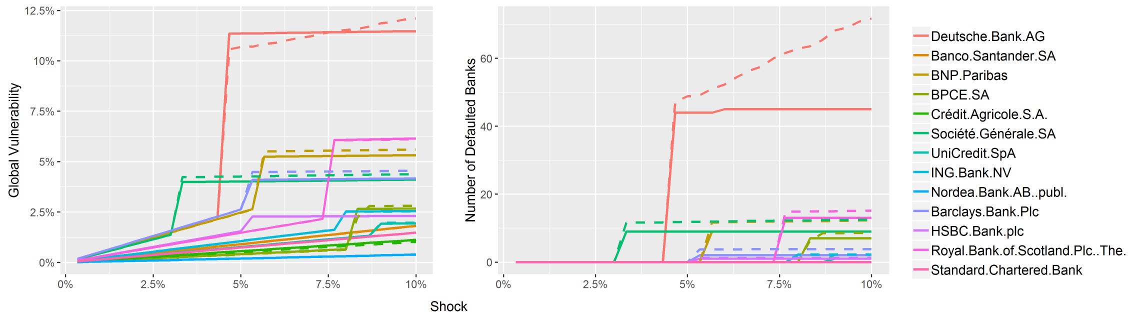

(b) RV

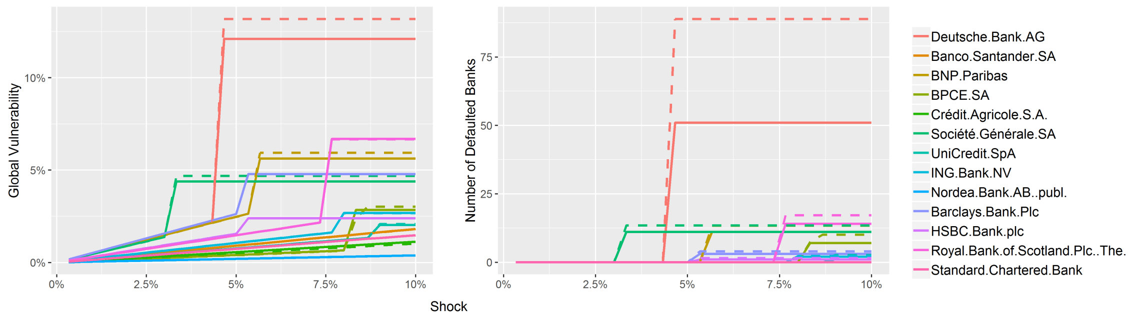

(c) DC

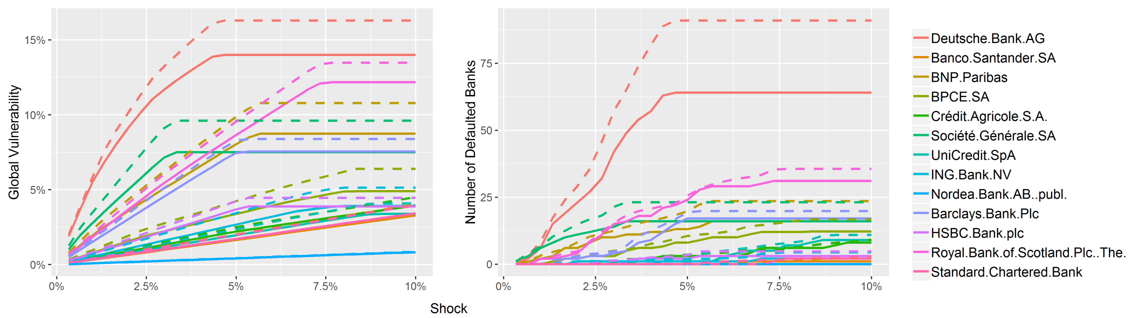

(d) aDR

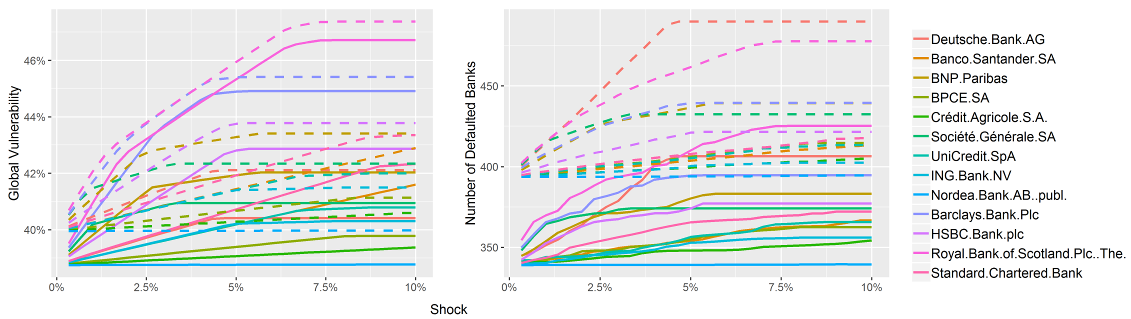

(e) cDR

Figure 10: Global vulnerability (left) and number of defaults (right) caused by shocking the G-SIBs separately with shock sizes ranging from 1% to 10% of external assets. Values of the networks with the original densities are pictured in dashed lines. Reported values are averages over 100 simulated networks (excluding the Rest-of-the-World node). Legends are ordered according to the respective global vulnerability at a shock size of 10%.

Next, we analyze shock scenarios where all banks are shocked equally with various shock sizes on external assets. The results are presented in Fig. 11 in comparison to the results of the same shock scenarios applied to the originally sparse networks. Interestingly, for the considered shock scenarios, global vulnerability does barley differ between the sparse and densly connected networks. However, we can observe an increase in the number of defaulting banks for networks with higher densities. This means that losses are distributed differently in both network sets. In the more densely connected networks contagion seems to flow across a bigger number of small nodes that at some point default and propagate their losses back to big nodes.

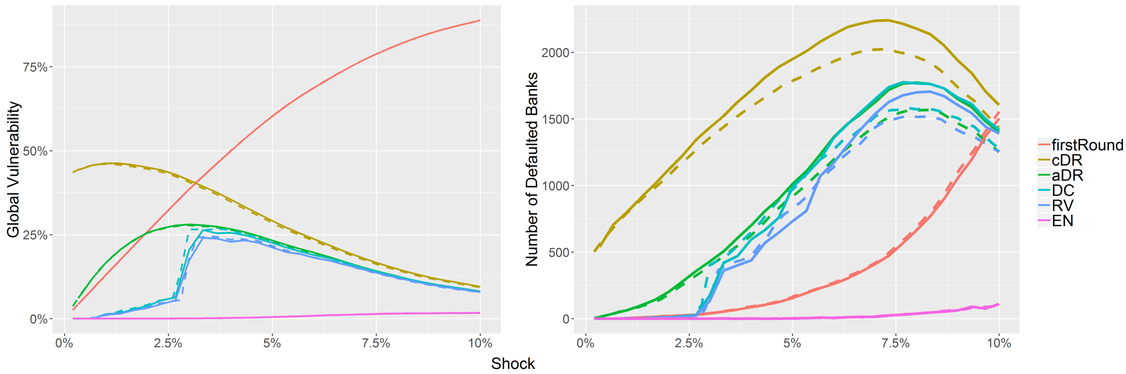

Figure 11: Global vulnerability (left) and number of defaults (right) caused by shocking all banks equally with shock sizes ranging from 1% to 10% of external assets. Values of the networks with the original densities are pictured in dashed lines. Reported values are averages over 100 simulated networks (excluding the Rest-of-the-World node).

7. Conclusion and outlook

Realistic models of inter-banking networks are necessary for an adequate and flexible assessment of systemic risk. Their construction, however, remains challenging, because of the very limited data availability. In this paper we contribute to this research topic by presenting a block-structured model that reconstructs inter-banking networks across multiple countries. The advantages of our model are the following. First of all, our model allows to incorporate structural differences in financial networks across countries and offers great flexibility via the block-structure. The density and the reciprocity can be chosen separately for every block. Likewise the constraints on the weights, i.e. row sums, column sums, and block-weights can be set separately. This allows users, like central banks or policy-makers, who might have partial access to additional information to calibrate the model more accurately. Also, in case further information on aggregated level becomes available in the future, it can easily be incorporated in our model. As a trade-off on accuracy of network reconstruction and data availability, our model is calibrated on a small number of input factors, that are able to induce important network characteristics. As shown in Section 5.2 the model correctly reproduces known aggregated characteristics of financial networks like sparsity, positive reciprocity, disassortativity, and short paths using only a small set of input factors. Moreover, we show how block-density, block-reciprocity, and block-weights, which might not be available explicitly, can be approximated. Since the calibration of the model is non trivial, we also present an algorithm to handle this task.

Finally, the simulated networks enable the application of a battery of contagion mechanisms and systemic risk measures. To demonstrate the potential of the model we conduct a systemic risk analysis on the reconstructed European interbank market. The results highlight the differences in systemic risk measures along five of the most prominent contagion models. Furthermore, the correlation between node characteristics and systemic risk caused by a bank's default as well the vulnerability suffered from the default of other banks is analyzed. We find that the loss that a bank's default causes on the interbank network is highly correlated with the number of its creditors (in-degree) as well as the amount borrowed (in-strength). Likewise, the vulnerability of a bank is highly correlated with the number of its debtors (out-degree) and the amount lend (out-strength). Among centrality measures, closeness centrality turns out to be the most significant for indicating systemic importance. In addition, the results on systemic risk are compared with the BCBS's ranking of global systemically important banks, which again turns out to depend heavily on the applied contagion model. Lastly, we can confirm earlier conclusions on the effect of the network density on systemic risk. Densely connected networks are more stable regarding small shocks and more fragile regarding big shocks when measured by the number of defaulting banks. The total loss in equity caused by big shocks, on the other hand, is not affected by the density of the network. These outcomes shed new light on systemic risk and its monitoring and can support policy-makers in their aim to stabilize the EU interbank market.

Appendix A.

Proof to Theorem 3.1 (Existence of a solution for the extended fitness model)
The detailed proof of Theorem 3.1 takes several pages and can be found in the supplementary information to this manuscrip, which is available from the corresponding author. Here we outline the main steps.

First, we substitute $y := r_{kl}^2 z_{kl} z_{lk}$. Second, we split the proof in two cases, depending on the values of $L_{kl}^{\leftrightarrow}, \tilde{L}_{kl}^{\rightarrow}$, and $\tilde{L}_{lk}^{\rightarrow}$. **Case 1**:

$$\begin{aligned}
L_{kl}^{\leftrightarrow} &\leq \sum_{i\in C_k, j\in C_l} \frac{s_i^{(out)} s_j^{(in)} s_j^{(out)} s_i^{(in)}}{s_i^{(out)} s_j^{(in)} + s_j^{(out)} s_i^{(in)} + s_i^{(out)} s_j^{(in)} s_j^{(out)} s_i^{(in)}},\\
\tilde{L}_{kl}^{\rightarrow} &\leq \sum_{i\in C_k, j\in C_l} \frac{s_i^{(out)} s_j^{(in)}}{s_i^{(out)} s_j^{(in)} + s_j^{(out)} s_i^{(in)} + s_i^{(out)} s_j^{(in)} s_j^{(out)} s_i^{(in)}},\\
\tilde{L}_{lk}^{\rightarrow} &\leq \sum_{i\in C_k, j\in C_l} \frac{s_j^{(out)} s_i^{(in)}}{s_i^{(out)} s_j^{(in)} + s_j^{(out)} s_i^{(in)} + s_i^{(out)} s_j^{(in)} s_j^{(out)} s_i^{(in)}}.
\end{aligned} \tag{A.1}$$

For Case 1, the existence of a solution is straight forward to prove with the Bolzano–Poincaré–Miranda theorem[11], where we define the parameter support by $(y, z_{kl}, z_{lk}) \in \left[m^{-1}, m\right]^3$, for $m \in \mathbb{R}_{>0}$ big enough.

Case 2: If the conditions of Case 1 are not satisfied, i.e. Eq. (A.1), choose $\alpha, \beta, \gamma \in \mathbb{R}_{>0}$ such that

$$\begin{aligned}
L_{kl}^{\leftrightarrow} &\leq \sum_{i\in C_k, j\in C_l} \frac{\gamma s_i^{(out)} s_j^{(in)} s_j^{(out)} s_i^{(in)}}{\alpha s_i^{(out)} s_j^{(in)} + \beta s_j^{(out)} s_i^{(in)} + \gamma s_i^{(out)} s_j^{(in)} s_j^{(out)} s_i^{(in)}},\\
\tilde{L}_{kl}^{\rightarrow} &\leq \sum_{i\in C_k, j\in C_l} \frac{\alpha s_i^{(out)} s_j^{(in)}}{\alpha s_i^{(out)} s_j^{(in)} + \beta s_j^{(out)} s_i^{(in)} + \gamma s_i^{(out)} s_j^{(in)} s_j^{(out)} s_i^{(in)}},\\
\tilde{L}_{lk}^{\rightarrow} &\leq \sum_{i\in C_k, j\in C_l} \frac{\beta s_j^{(out)} s_i^{(in)}}{\alpha s_i^{(out)} s_j^{(in)} + \beta s_j^{(out)} s_i^{(in)} + \gamma s_i^{(out)} s_j^{(in)} s_j^{(out)} s_i^{(in)}},
\end{aligned} \tag{A.2}$$

holds. Analogously to Case 1, it follows from the Bolzano–Poincaré–Miranda theorem that there exists a solution $\left(y^*, z_{kl}^*, z_{lk}^*\right) \in \left[m^{-1}, m\right]^3$, and hence, $\left(z_{kl}^* \alpha\right)$, $\left(z_{lk}^* \beta\right)$, and $(y^* \gamma)$ constitutes a solution w.r.t. the original equations. The existence of $\alpha, \beta, \gamma \in \mathbb{R}_{>0}$ from Eq. (A.2) can be proved in several steps using the intermediate value theorem and the implicit function theorem.

Proof of Theorem 3.2 (Uniqueness of a solution for the extended fitness model)
Consider the ERGM defined by maximizing the Shannon entropy such that the expected particular degree sequences of Eqs. (19) to (22) and the expected number of reciprocal links $L_{kl}^{\leftrightarrow}$ are satisfied. A solution to

[11] See for example [49], Theorem 2, and [34], and the references therein.

this ERGM is given by

$$e^{-\lambda_i^{(out,k)}} := \sqrt{z_{kl}}s_i^{(out,k)}, \quad \text{for all } i \in C_k \tag{A.3}$$
$$e^{-\lambda_i^{(in,k)}} := \sqrt{z_{kl}}s_i^{(in,l)}, \quad \text{for all } i \in C_l \tag{A.4}$$
$$e^{-\lambda_i^{(out,l)}} := \sqrt{z_{lk}}s_i^{(out,l)}, \quad \text{for all } i \in C_l \tag{A.5}$$
$$e^{-\lambda_i^{(in,l)}} := \sqrt{z_{lk}}s_i^{(in,k)}, \quad \text{for all } i \in C_k \tag{A.6}$$
$$e^{-\lambda_r} := r, \tag{A.7}$$

where the λ's denote the corresponding Lagrange multipliers. From the general theory of maximum entropy problems, we know that the solving probability distribution is unique, see for example [18]. This means that all link probabilities, as given by Eqs. (6) to (8), are unique, see [24]. From this it obviously follows that z_{kl}, z_{lk}, and r are unique. □

Proof of Theorem 3.3 (Uniqueness of a solution for the ERGM)
From the general theory of maximum entropy problems, we know that the solving probability measure is unique, see for example [18]. Let's assume there exists a second set of parameters $\tilde{\theta}$ solving the ERGM, i.e. defining the same probability measure. This especially means that $p_\theta(w) = p_{\tilde{\theta}}(w)$ for all $w \in \mathcal{G}_a$. Let $w^{(0)}$ denote the graph where all $w_{ij}^{(0)} = 0$, then we get

$$\begin{aligned} & p_\theta(w^{(0)}) &&= p_{\tilde{\theta}}(w^{(0)}) \\ \Leftrightarrow\quad & Z_\theta^{-1} \underbrace{e^{-H_\theta(w^{(0)})}}_{=1} &&= Z_{\tilde{\theta}}^{-1} \underbrace{e^{-H_{\tilde{\theta}}(w^{(0)})}}_{=1} \\ \Leftrightarrow\quad & Z_\theta &&= Z_{\tilde{\theta}}. \end{aligned}$$

Let $w^{(a,b)}$ denote the graph where all elements are 0 and $w_{ab}^{(a,b)} = 1$, then we get

$$\begin{aligned} & p_\theta(w^{(a,b)}) &&= p_{\tilde{\theta}}(w^{(a,b)}) \\ \Leftrightarrow\quad & Z_\theta^{-1} \underbrace{e^{-H_\theta(w^{(0)})}}_{=\exp(-\theta_{ab})} &&= Z_{\tilde{\theta}}^{-1} \underbrace{e^{-H_{\tilde{\theta}}(w^{(0)})}}_{=\exp\left(-\tilde{\theta}_{ab}\right)} \\ \Leftrightarrow\quad & \theta_{ab} &&= \tilde{\theta}_{ab}. \end{aligned}$$

Hence, it follows that all sums $\theta_{ij} = \left(\theta_i^{(out)} + \theta_j^{(in)} + \theta_{ij}^{(block)}\right)$ are unique for all $i, j = 1, \ldots, n$ where $a_{ij} = 1$. □

References

[1] D. Acemoglu, A. Ozdaglar, and A. Tahbaz-Salehi. Systemic Risk and Stability in Financial Networks. *American Economic Review*, 105(2):564–608, 2015.

[2] F. Allen and D. Gale. Financial contagion. *Journal of Political Economy*, 108(1):1–33, 2000.

[3] E. I. Altman and V. M. Kishore. Almost Everything You Wanted to Know about Recoveries on Defaulted Bonds. *Financial Analysts Journal*, 52(6), 1996.

[4] K. Anand, B. Craig, and G. Von Peter. Filling in the blanks: Network structure and interbank contagion. *Quantitative Finance*, 15(4):625–636, 2015.

[5] K. Anand, I. van Lelyveld, A. Banai, T. C. Silva, S. Friedrich, R. Garratt, G. Halaj, I. Hansen, B. Howell, H. Lee, S. Martínez Jaramillo, J. Molina-Borboa, S. Nobili, S. Rajan, S. R. Stancato de Souza, D. Salakhova, and L. Silvestri. The missing links: A global study on uncovering financial network structures from partial data. *Journal of Financial Stability*, 2017.

[6] P. Baral and J. Fique. Estimation of bilateral connections in a network: copula vs.maximum entropy. *Mimeo*, 2012.

[7] M. Bardoscia, S. Battiston, F. Caccioli, and G. Caldarelli. DebtRank: A microscopic foundation for shock propagation. *PLoS ONE*, 10(6), 2015.

[8] L. Bargigli, G. Di Iasio, L. Infante, F. Lillo, and F. Pierobon. The multiplex structure of interbank networks. *Quantitative Finance*, 15(4):673–691, 2015.

[9] S. Battiston, G. Caldarelli, M. D'Errico, and S. Gurciullo. Leveraging the network : a stress-test framework based on DebtRank. Statistics and Risk Modeling. *Statistics Risk Modeling*, 33(3–4), 2016.

[10] S. Battiston, D. Delli Gatti, M. Gallegati, B. Greenwald, and J. E. Stiglitz. Default cascades: When does risk diversification increase stability? *Journal of Financial Stability*, 8(3):138–149, 2012.

[11] S. Battiston, M. Puliga, R. Kaushik, P. Tasca, A. Vespignani, and G. Caldarelli. DebtRank: Too Central to Fail? Financial Networks, the FED and Systemic Risk. *Scientific Reports*, 2(541), 2012.

[12] G. Caldarelli, A. Capocci, P. De Los Rios, and M. Muñoz. Scale-free networks from varying vertex intrinsic fitness. *Phys. Rev. Lett.*, 89, 2002.

[13] E. Cerutti, S. Claessens, and P. McGuire. Systemic Risks in Global Banking: What Available Data can tell us and What More Data are needed? Working Paper 11/222, International Monetary Fund, 2011.

[14] R. Cifuentes, H. S. Shin, and G. Ferrucci. Liquidity risk and contagion. *Journal of the European Economic Association*, 3(2–3):556–566, 2005.

[15] G. Cimini, T. Squartini, A. Gabrielli, and D. Garlaschelli. Estimating topological properties of weighted networks from limited information. *Phys. Rev. Lett. E*, 92(040802(R)), 2015.

[16] G. Cimini, T. Squartini, D. Garlaschelli, and A. Gabrielli. Systemic risk analysis on reconstructed economic and financial networks. *Scientific Reports*, 5, 2015.

[17] R. Cont, A. Moussa, and E. B. Santos. *Network structure and systemic risk in banking systems*, page 327–367. Cambridge University Press, 2013.

[18] T. M. Cover and J. A. Thomas. *Elements of Information Theory*. Wiley-Interscience, 2006.

[19] B. Craig and G. Von Peter. Interbank tiering and money center banks. *Journal of Financial Intermediation*, 23(3):322–347, 2014.

[20] P. De Bandt and O. Hartmann. Systemic risk: A survey. Working Paper 35, European Central Bank, Frankfurt, Germany, 2000.

[21] M. Drehmann and N. Tarashev. Measuring the systemic importance of interconnected banks. *Journal of Financial Intermediation*, 2:586–607, 2013.

[22] L. Eisenberg and T. H. Noe. Systemic risk in financial systems. *Management Science*, 47(2):236–249, 2001.

[23] H. Elsinger, A. Lehar, and M. Summer. *Network models and systemic risk assessment*, volume 48, page 287–305. Cambridge University Press, 2013.

[24] J. Engel, M. Scherer, and A. Pagano. Reconstructing the topology of financial networks from degree distributions and reciprocity. *forthcoming in the Journal of Multivariate Analysis*, 2019.

[25] A. Gandy and L. A. M. Veraart. A Bayesian methodology for systemic risk assessment in financial networks. *Management Science*, 2016.

[26] A. Gandy and L. A. M. Veraart. Adjustable Network Reconstruction with Applications to CDS Exposures. 2017.

[27] D. Garlaschelli and M. I. Loffredo. Patterns of link reciprocity in directed networks. *Phys. Rev. Lett.*, 93, 2004.

[28] D. Garlaschelli and M. I. Loffredo. Generalized Bose-Fermi statistics and structural correlations in weighted networks. *Phys. Rev. Lett.*, 102, 2009.

[29] G. Hałaj and C. Kok. Assessing interbank contagion using simulated networks. Working Paper 1506, European Central Bank, 2013.

[30] P. W. Holland and S. Leinhardt. An Exponential Family of Probability Distributions for Directed Graphs. *Journal of the American Statistical Association*, 76(373):33–50, 1981.

[31] A.-C. Hüser. Too interconnected to fail: A survey of the interbank networks literature. *Journal of Network Theory in Finance*, 1(3):1–50, 2015.

[32] D. Lusher, J. Koskinen, and G. Robins. *Exponential Random Graph Models for Social Networks: Theory, Methods, and Applications*. Cambridge University Press, 2012.

[33] R. Mastrandrea, T. Squartini, G. Fagiolo, and D. Garlachelli. Enhanced reconstruction of weighted networks from strengths and degrees. *New Journal of Physics*, 16, 2014.

[34] J. Mawhin. Variations on Poincaré–Miranda's theorem. *Advanced Nonlinear Studies*, 13, 2013.

[35] P. Mazzarisi and F. Lillo. *Methods for Reconstructing Interbank Networks from Limited Information: A Comparison*, page 201–215. Springer International Publishing, Cham, 2017.

[36] P. E. Mistrulli. Assessing financial contagion in the interbank market: Maximum entropy versus observed interbank lending patterns. *Banca d'Italia, Temi di discussione*, (641), 2007.

[37] N. Musmeci, S. Battiston, G. Caldarelli, M. Puliga, and A. Gabrielli. Bootstrapping topological properties and systemic risk of complex networks using the fitness model. *Journal of Statistical Physics*, 151:720–734, 2013.

[38] M. E. J. Newman. *Networks An Introduction*. Oxford University Press, 2010.

[39] Basel Committee on Banking Supervision. Basel III: A global regulatory framework for more resilient banks and banking

systems Bank for International Settlements. 2010.

[40] Basel Committee on Banking Supervision. Making supervisory stress tests more macroprudential: Considering liquidity and solvency interactions and systemic risk. *BIS Working Paper*, 2015.

[41] Basel Committee on Banking Supervision. Making supervisory stress tests more macroprudential: Considering liquidity and solvency interactions and systemic risk. BCBS Working Papers 29, Bank for International Settlements, 2015.

[42] J. Park and M. E. J. Newman. The statistical mechanics of networks. *Phys. Rev.*, 70, 2004.

[43] L. C. G. Rogers and L. A. M. Veraart. Failure and Rescue in an Interbank Network. *Management Science*, 59(4):882–898, 2013.

[44] A. Roncoroni, S. Battiston, M. D'Errico, G. Hałaj, and C. Kok. Interconnected Banks and Systemically Important Exposures. 2018.

[45] T. Roukny, C.-P. Georg, and S. Battiston. A network analysis of the evolution of the German interbank market. Discussion Paper 22, Deutsche Bundesbank, 2014.

[46] V. D. P. Servedio, G. Caldarelli, and A. Buttà. Vertex intrinsic fitness: How to produce arbitrary scale-free networks. *Phys. Rev. E*, 70(056126), 2004.

[47] T. A. B. Snijders, P. E. Pattison, G. L. Robins, and M. S. Handcock. New specifications for exponential random graph models. *Sociological methodology*, 36(1):99–153, 2006.

[48] T. Squartini and D. Garlaschelli. Analytical maximum-likelihood method to detect patterns in real networks. *New J. Phys.*, 13, 2011.

[49] M. Turzański. The Bolzano–Poincaré–Miranda theorem – discrete version. *Topology and its Applications*, 159(13):3130–3135, 2012.

[50] C. Upper. Simulation methods to assess the danger of contagion in interbank markets. *Journal of Financial Stability*, 7:111–125, 2011.

[51] C. Upper and A. Worm. Estimating bilateral exposures in the german interbank market: Is there a danger of contagion? *European Economic Review*, 48:827–849, 2004.

[52] G. Visentin, S. Battiston, and M. D'Errico. Rethinking financial contagion. 2016.